

NASA CR- 177877

TYPE III FINAL REPORT FOR PERIOD
16 OCTOBER 1984 TO 15 APRIL 1986

CONTRACTS: NASS-28609
(NASS-23761)

THE GAMMA-RAY SPECTROMETER EXPERIMENT
ON THE SOLAR MAXIMUM MISSION SATELLITE

(NASA-Cr-177877) THE GAMMA-RAY SPECTROMETER N87-13394
EXPERIMENT ON THE SOLAR MAXIMUM MISSION
SATELLITE Final Report, 16 Oct. 1984 - 15
Apr. 1986 (New Hampshire Univ.) 67 p
CSCS 03B G3/93 44633
Unclas

UNIVERSITY OF NEW HAMPSHIRE
DEPARTMENT OF PHYSICS
DURHAM, NH 03824

Prepared by
GAMMA-RAY ASTRONOMY GROUP
PHYSICS DEPARTMENT
UNIVERSITY OF NEW HAMPSHIRE

PRINCIPAL INVESTIGATOR: E. L. CHUPP

Prepared for
GODDARD SPACE FLIGHT CENTER
GREENBELT, MARYLAND 20771

15 APRIL 1986

TITLE TYPE III FINAL REPORT
CONTRACTS 28609 & 25731

SUBMITTED BY UNIVERSITY OF NEW HAMPSHIRE
DURHAM, NEW HAMPSHIRE 03824

PRINCIPAL INVESTIGATOR EDWARD L. CHUPP
DEPARTMENT OF PHYSICS
UNIVERSITY OF NEW HAMPSHIRE
603/862-2750 (OFFICE)
603/868-2514 (HOME)
SS # [REDACTED]

PROJECT SCIENTIST DAVID J. FORREST
DEPARTMENT OF PHYSICS
UNIVERSITY OF NEW HAMPSHIRE
603/862-2750 (OFFICE)
603/868-2480 (HOME)
SS # [REDACTED]

DOCUMENT PREPARED BY W. THOMAS VESTRAND
DEPARTMENT OF PHYSICS
UNIVERSITY OF NEW HAMPSHIRE
603/862-2750 (OFFICE)
603/942-5467 (HOME)
SS # [REDACTED]

DATE SUBMITTED APRIL 15, 1986

W. Thomas Vestrand 3/12/86

W. THOMAS VESTRAND DATE
RESEARCH SCIENTIST

David J. Forrest 3/12/86

DAVID J. FORREST DATE
PROJECT SCIENTIST

Edward L. Chupp 86/3/13

EDWARD L. CHUPP DATE
PRINCIPAL INVESTIGATOR

TABLE OF CONTENTS

1. INTRODUCTION.....1

 1.1. HISTORY OF PROJECT AND PURPOSE OF GRS.....1

 1.2. BRIEF OVERVIEW OF MAJOR RESULTS.....3

2. INSTRUMENT DESCRIPTION AND SCIENTIFIC OBJECTIVES.....5

3. BRIEF SUMMARY OF MAJOR RESULTS.....7

 3.1. SOLAR BURSTS.....7

 3.1.1. TIMING STUDIES.....7

 3.1.2. NARROW NUCLEAR LINES.....10

 3.1.3. BROAD BAND NUCLEAR EMISSION.....11

 3.1.4. NEUTRON CAPTURE LINE.....12

 3.1.5. POSITRON ANNIHILATION LINE.....14

 3.1.6. HIGH-ENERGY GAMMA-RAY AND NEUTRON EMISSION ...15

 3.1.7. DIRECTIVITY OF THE CONTINUUM EMISSION.....19

 3.1.8. EVIDENCE FOR PERIODICITY.....21

 3.1.9. COMPARISON OF GRS GAMMA RAYS WITH OTHER
 FLARE EMISSIONS.....21

 3.2. COSMIC GAMMA-RAY BURSTS.....23

 3.2.1. BROAD BAND SPECTRAL FITS.....24

 3.2.2. SEARCH FOR POSITION ANNIHILATION FEATURES.....25

 3.2.3. HARDNESS RATIOS.....25

 3.2.4. SEARCH FOR LONGER DURATION EVENTS.....26

 3.3. "STEADY" SOURCES26

 3.3.1. GALACTIC ²⁶Al.....27

 3.3.2. GALACTIC POSITRON ANNIHILATION27

 3.3.3. SEARCH FOR SPECIFIC TRANSIENTS.....28

 3.3.4. SS433.....28

 3.3.5. NOVAE29

4. DATA PROCESSING AND ANALYSIS.....29

 4.1. OVERALL DATA PROCESSING RESPONSIBILITIES.....29

 4.2. UNH DATA ANALYSIS PROGRAM AND DOCUMENTATION PLANS....30

5. NATIONAL SPACE DATA AND DOCUMENTATION CENTER
 PLANS (NSDDC).....32

6. GUEST INVESTIGATOR PROGRAM.....34

7. AIR FORCE TASKS.....35
8. REFERENCES.....37
APPENDIX A.....A1
APPENDIX B.....B1
APPENDIX C.....C1

LIST OF TABLES AND FIGURES

	PAGE
Figure 1.	Schematic drawing of the gamma-ray spectrometer (GRS) experiment showing the major subsystem components in top and cross-sectional side views. 6a
Figure 2.	GRS inflight calibration in the X-ray detectors #1 and #2 on days of year 173/1980 and 115/1984 respectively. 6c
Figure 3.	GRS high-energy monitor (HEM) inflight calibration gain factor from launch, 1980 February 14 to 1984 April 24. 6d
Figure 4.	Main channel gamma-ray spectrometer inflight calibration ^{60}Co pulse height spectra for days of year 173/1980 and 116/1984 respectively. 7a
Figure 5.	Main channel background spectra accumulated over a 3-year interval. 7b
Figure 6.	A comparison of the extremes of duration, the rise time, and the burst width for two impulsive flares in gamma-ray emission at 4.1-6.4 MeV (from Forrest 1983). 8a
Figure 7.	The time history of photon emissions from 40 keV to ~ 25 MeV is shown for the flare on 1982 February 8, which occurred before 1249 UT. Early in the flare, low-energy photons $\gtrsim 300$ keV are occulted by the Earth's atmosphere. The times of the peak intensity for the pulse at ~ 1250 UT are the same within 2 s for all photon energies. 9a
Figure 8.	The time-integrated excess gamma-ray counts spectrum above background (solid curve), after removal of a bremsstrahlung continuum, is shown for the 1981 April 27 flare (Forrest et al. 1983). Significant gamma-ray line features and their origin are (1) 6.129 MeV (^{16}O); (2) 4.439 MeV (^{12}C); (3) 2.313 MeV (^{14}N) and 2.223 MeV ($n\gamma$); (4) 1.634 MeV (^{20}Ne); (5) 1.369 MeV (^{24}Mg) and 1.238 MeV (^{56}Fe); and (6) 511 keV (β^+), 478 keV (^7Li), and 431 keV (^7Be). The 2.223-MeV line, normally the strongest for disk flares, is strongly suppressed in this limb flare. The dotted curve is based on a predicted incident photon spectrum folded through the instrument response. The incident spectrum was generated assuming an accelerated ion spectrum of the form $\alpha T = 0.02$, incident on an ambient thick target with "standard" photospheric abundances (Ramaty et al. 1983). 10a
Figure 9.	The fluence (total time-integrated flux) of γ -ray > 270 keV is compared with the 4-8 MeV excess for GRS events observed between 1980 February and 1982 February (from Forrest 1983). 11a

		PAGE
Figure 10a.	The (10-140) MeV photon spectrum for the impulsive phase of the 1980 June 21 flare (Forrest et al. 1985)	15a
Figure 10b.	The (10-140) MeV photon spectrum for the impulsive phase of the 1982 June 3 flare (Forrest et al. 1985)	15a
Figure 10c.	The (10-140) MeV photon spectrum early in the extended phase of the 1982 June 3 flare (Forrest et al. 1985)	15a
Figure 10d.	The (10-140) MeV spectrum showing the photon spectrum and the effects of the high-energy neutrons in the extended phase of the 1982 June 3 flare (Forrest et al. 1985)	15a
Figure 11.	The arrival time history of energetic photons > 25 MeV and neutrons at the Earth is shown for the intense flare on 1980 June 21, as recorded by the GRS (Chupp et al. 1982)	18a
Figure 12.	The percentage of limb events is shown for gamma-ray flares (GRS) detected between February 1980 and December 1982. Three control samples: GOES events, HXRBS events, and H α flares, are also illustrated. The control samples were selected from only that subset of the events that occurred when the GRS was capable of detecting a coincident event.	19a
Figure 13.	Energetic solar flare events with photon emission above 300 keV are illustrated by short vertical lines, plotted versus time for successive years of observation after the Gamma-Ray Spectrometer (GRS) began operation.	21a
Figure 14.	Time histories for the 1982 March 1 event. The time dependence of the hardness ratio is also illustrated (Norris et al. 1985)	25a
Figure 15.	Variation in the intensity of a line at 1.81 MeV obtained when data from times > 10,000 s from the last SAA passage in the 1.6-2.0 MeV range are fit by a power-law continuum and lines at 1.75 and 1.81 MeV. The gradual increase in the 1.81 MeV intensity is due to the nearby ^{22}Na line which is not resolved in this two line fit. Sky-viewing data (zenith angle < 72 $^{\circ}$).	27a
Figure 16.	Light curves of the Doppler shifted \sim 1.37 MeV gamma-ray line data from the SS433. HEAO-3 data (stars), SMM data (unfilled circles). a) blue beam, b) red beam. c) 2695 MHz radio light curve for SS433 (Geldzahler et al. 1985)	29a
Figure 17.	SMM GRS Data Processing Flow Diagram.	31a

Table 1.	SMM GRS Gamma Ray Spectrometer Team.	2
Table 2.	Summary of the Gamma-Ray Spectrometer Experiment Scientific Capabilities.	6b

ACKNOWLEDGEMENTS

During the period covered by this report, many people contributed to the scientific effort of the SMM GRS experiment. Here we only wish to single out those colleagues and co-workers who significantly contributed data for the preparation of this Report. We thank, at the Naval Research Laboratory, Gerry Share; and at the Max-Planck Institute, Erich Rieger for their contributions. Of the many whose data analysis made this effort possible, we would especially like to thank Sabrina Kirwan and Karen Dowd. For his part documenting the data analysis procedure, we thank Ken Levenson. We also acknowledge Lauree Miller and Cathy Paquette for typing. Our special appreciation goes to Mary Chupp for her tireless effort in editing and assembling this document.

PREFACE

On 1980 February 14 the SMM satellite was launched with a Gamma-Ray Spectrometer (GRS) on board. The instrument was selected for this mission through the NASA Announcement of Opportunity Process. During the six years following launch, the instrument has functioned without interruption and with no detectable degradation.

This document covers work in the contractual period 16 October 1984 to 15 April 1986 for contract NASS-28609; however much of the work reported here has begun immediately after launch. The work performed in the period from 14 February 1980 through 15 October 1984 was covered by contract NASS-23761 and has been described in a Type III Final Report submitted to NASA on March 22, 1986. For completeness, this report summarizes work since launch.

In the following we briefly report on the discoveries made by SMM GRS during the past six years. Also, we describe some of the research currently being done by the SMM GRS team and some of the work that will be undertaken in the future.

Some of the major discoveries made by GRS are:

1. High-energy ions and relativistic electrons can be accelerated by flares in only a few seconds.
2. Relativistic electron and energetic ion acceleration is a relatively common process in flares.
3. The first direct detection of energetic solar neutrons.
4. A gamma-ray spectrum from a limb solar flare which has over 25 nuclear lines never seen before from any cosmic source.
5. The high-energy electrons which generate the bremsstrahlung continuum have a directed distribution.
6. Flares occur with a period of ~ 55 days.

7. Cosmic gamma-ray bursts, as a class, produce photons with energies > 1 MeV.
8. A strong line at ~ 1.8 MeV from ^{26}Al which is produced by nucleosynthesis in our galaxy.

1. INTRODUCTION

1.1. HISTORY OF PROJECT AND PURPOSE OF GRS

The Gamma-Ray Spectrometer[•] (GRS) on the SMM satellite was built by the University of New Hampshire (UNH), Durham, New Hampshire, and the Max Planck Institute for Extraterrestrial Physics (MPE) in Garching, West Germany. Subcontractor support was provided to these two institutions by American Science and Engineering (AS&E) in Cambridge, Massachusetts and by Messerschmidt, Bolkow and Blohn (MBB) in Munich, West Germany. The two research institutions, UNH and MPE, along with the Naval Research Laboratory (NRL) were assigned the responsibility for joint data analysis, after the experiment selection in 1976. The Principal Investigator Institute is UNH. Table 1. lists the current scientific investigators for the overall scientific effort. This report describes the UNH data analysis effort and scientific results obtained since launch on 1980 February 14 to the end of the contracting period 1986 April 15. The scientific results described in Section 3.0 are the result of the collective efforts of the three collaborating institutions referred to as the SMM GRS Team. Analysis of the primary SMM GRS data-base is ongoing at all three institutions.

• The instrument was formerly called the Gamma-Ray Experiment with the acronym GRE, but this was changed after launch to GRS to be in line with the style for other SMM instruments.

Table 1. SMM GRS Gamma-Ray Spectrometer Team

**SMM GRS
GAMMA RAY SPECTROMETER TEAM**

UNIVERSITY OF NEW HAMPSHIRE

E. L. CHUPP - PRINCIPAL INVESTIGATOR
DAVID J. FORREST - PROJECT SCIENTIST
STEVEN M. MATZ (Thesis completed March, 1986)
JANAKI NARAYANASWAMY
W. THOMAS VESTRAND

MAX PLANCK INSTITUTE (GARCHING)

GOTTFRIED KANBACH
ERICH REIGER
CLAUS REPPIN

NAVAL RESEARCH LABORATORY

BARRY GELDZAHLER
ROBERT KINZER
DANIEL MESSINA
GERALD SHARE

GUEST INVESTIGATORS

EDWARD CLIVER (AFGL)
*CAROL CRANNELL (GSFC)
*SHARAD KANE (UCB)
THOMAS PRINCE (CIT)
*REUVEN RAMATY (GSFC)
*RICHARD SCHWARTZ (JPL)

CURRENT GUEST INVESTIGATORS

+CAROL JO CRANNELL
+ROBERT DECKER
+BARRY GELDZAHLER
+MUKUL KUNDU
+KENNETH LANG
+MARK PESSES
+DEAN SMITH

*Funded by NASA under Guest Investigator Program 1984-1985
+Funded by NASA under Guest Investigator Program 1985-1986

1.2. BRIEF OVERVIEW OF MAJOR RESULTS

Solar flares are huge, explosive releases of energy at the Sun. Flares may last from 10 minutes to hours, producing electromagnetic radiation from radio waves, through optical frequencies and up to gamma-rays. This represents a spectral band more than thirteen orders of magnitude wide. In addition, energetic particles accelerated by flares are observed in space. Large flares can release thousands of times more energy in radiation and in particles than is consumed in the United States in one year.

It is generally believed that this energy is stored in magnetic fields at or near sunspots. Although flares are quite common and are intensely studied, the mechanisms by which this energy is released and converted into the forms we observe remains unknown. The Solar Maximum Mission satellite (SMM), was designed to make comprehensive observations of solar flares over a wide range of electromagnetic frequencies and thereby provide new clues about the flaring process.

In this report, we concentrate on observations by the Gamma-Ray Spectrometer (GRS) on the SMM satellite. This detector system is sensitive to high-energy X-rays, gamma-rays, and energetic neutrons. These neutral quanta provide a probe of the highest energy processes in a flare. The quanta are produced by energetic collisions of protons and nuclei, radioactive decay, particle-antiparticle annihilation, and thermonuclear reactions.

Prior to SMM only a few solar flares had been detected at gamma-ray energies. Based on these early data, theoreticians developed a picture of flares as taking place in two steps, with the highest energy electrons and ions accelerated slowly, minutes after impulsive low-energy electrons. It was also thought that the second step (viz. energetic ion and relativistic electron acceleration) might not occur in all flares.

The data from SMM GRS have dramatically altered this picture. The GRS has recorded over 150 flares since launch. These data conclusively show that both ions and electrons can be accelerated to very high energies within a few seconds. Furthermore, high-energy ion acceleration is much more common than previously thought. Indeed, our data are consistent with the hypothesis that energetic ions are accelerated in all flares.

In the large flare of 1981 April 27, we measured a spectrum rich in gamma-ray lines, most never before seen from the Sun. These lines all indicate the collision of high-energy ions with nuclei in the solar atmosphere. The measured spectrum seems to conflict with the best predictions. In fact, the relative intensities of some lines differ by more than a factor of two from their predicted levels. The most likely explanation is that the abundances of certain heavy nuclei in the chromosphere are much different than previously thought.

The gamma-ray spectrometer also made the first direct detection of energetic neutrons from the Sun. The neutrons are thought to be produced by collisions of protons and nuclei at the Sun. Working back from the observed

arrival times we find that protons had to be accelerated to more than one thousand million electron volts (10^3 MeV) within seconds of the start of the flare.

In addition to the solar discoveries, the SMM GRS has made important discoveries about cosmic gamma-ray sources. First, from GRS observations, cosmic gamma-ray bursts are now known to have spectra that extend beyond 1 MeV. So far there are few theoretical explanations for this very energetic emission. Second, analysis of GRS data has shown the presence of the expected ^{26}Al gamma-ray line at ~ 1.81 MeV from the Galactic Disk. This gamma-ray line is a direct indicator of nucleosyntheses in our galaxy. Thus, although the GRS is part of a dedicated solar mission, it is also able to contribute to other areas of astrophysics because of its high sensitivity, stability, and large field-of-view.

2. INSTRUMENT DESCRIPTION AND SCIENTIFIC OBJECTIVES

The Gamma-Ray Spectrometer (GRS) represents an evolutionary step forward from an earlier gamma-ray instrument in the rotating wheel compartment of OSO-7. The main differences between the two instrument designs are:

- A large increase in the detector size allowed by the increased SMM spacecraft capabilities compared to the OSO-7 satellite dimensions. Specifically, the incorporation of seven 7.6 cm X 7.6 cm NaI (Tl) detectors, instead of the one detector on OSO-7.
- The incorporation of an automatic gain-servo loop, which had been developed at UNH in the early 1970's.

- The incorporation of a high-energy monitor (HEM) to record gamma rays and neutrons with energies > 10 MeV.
- GRS spectra were recorded with 16.384 s time resolution rather than the 180 s in OSO-7. In addition, the GRS observes the Sun continuously whereas the OSO-7 instrument had a 25% observing duty cycle.

The basic design of the actively shielded 7-sensor array is shown in Figure 1. For a detailed description of the instrument see Appendix A. Note that with the auxiliary X-ray detectors, the line spectrometer, and the high-energy monitor (HEM), the GRS instrument covers a photon energy band of more than four orders of magnitude (see Table 2.).

The GRS instrument was turned on approximately one week after the SMM launch in 1980 February. The instrument has functioned flawlessly and, except for satellite turn off, has continued to operate without interruption. Instrument monitoring and housekeeping data have shown no failures in any portion of the detector and no significant degradation of any of its scientific properties.

We illustrate several aspects of the stability and successful operation of the GRS instruments in the following figures showing results from the instrument's inflight calibration (IFC). Figure 2 shows the recorded 60 keV spectra from an on board ^{241}Am ($T_{1/2} = 433$ yrs) source as observed with the two X-ray monitors. The two sets of data were taken 4 years apart on 1980 June 21 and 1984 April 25. These two spectra show no change in X-ray detector sensitivity and only a small ($\sim 10\%$) change in the gain over the 4-year interval. Figure 3 shows the high-energy monitor's (HEM) gain changes over this same 4-year interval. Again, there is no evidence for

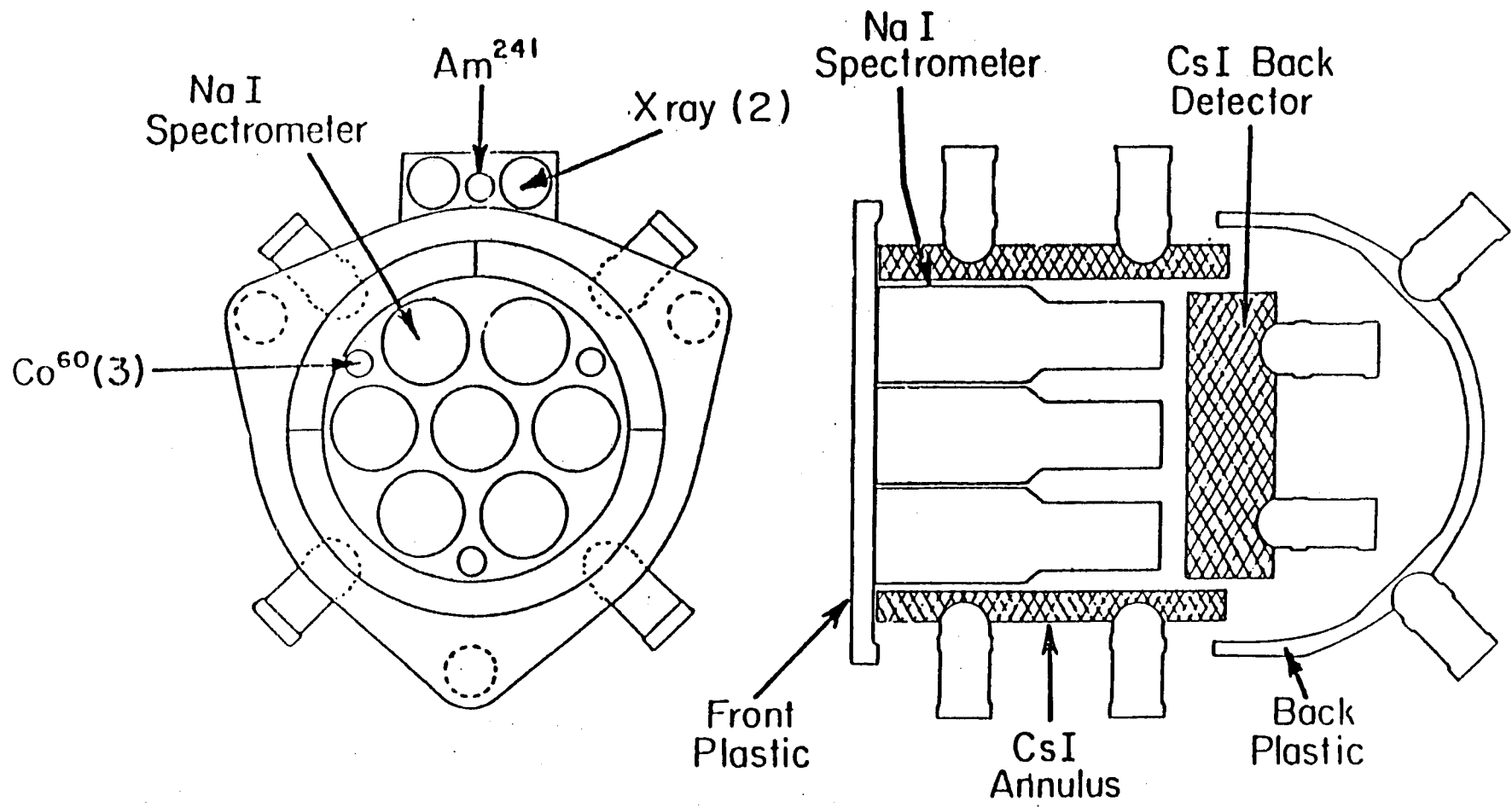


Figure 1. Schematic drawing of the gamma-ray spectrometer (GRS) experiment showing the major subsystem components in top and cross-sectional side views.

Table 2. Summary of the Gamma-Ray Spectrometer Experiment Scientific Capabilities

	Gamma-Ray Spectrometer	Gamma-Ray	High-Energy	Neutron	X1	X-Ray	X2
Energy Range	0.3-9 MeV	10-100 MeV		≥ 20 MeV		10-80 keV	25-140 keV
Energy Resolution	$\Delta E/E = 7\%$ FWHM at 0.662 MeV	$\Delta E/E \sim 1$		—		$\Delta E/E \sim 1$	
Effective Area	50-300 cm ²	~ 250 cm ²		~ 50 cm ²		8 cm ²	
Temporal Resolution	16.38 s full range 2.05 s 3.5-6.5 MeV 64 ms 0.30-0.35 MeV	2.05 s		2.05 s		1.0 s	
Typical Solar Flare Flux Sensitivity (cm ⁻² s ⁻¹)	$F(>0.3 \text{ MeV}) > \gamma\text{cm}^{-2}$	$F(>10 \text{ MeV}) > 0.02 \gamma\text{cm}^{-2}$		—		$F(>20 \text{ keV}) > 0.1 \gamma\text{cm}^{-2}$	

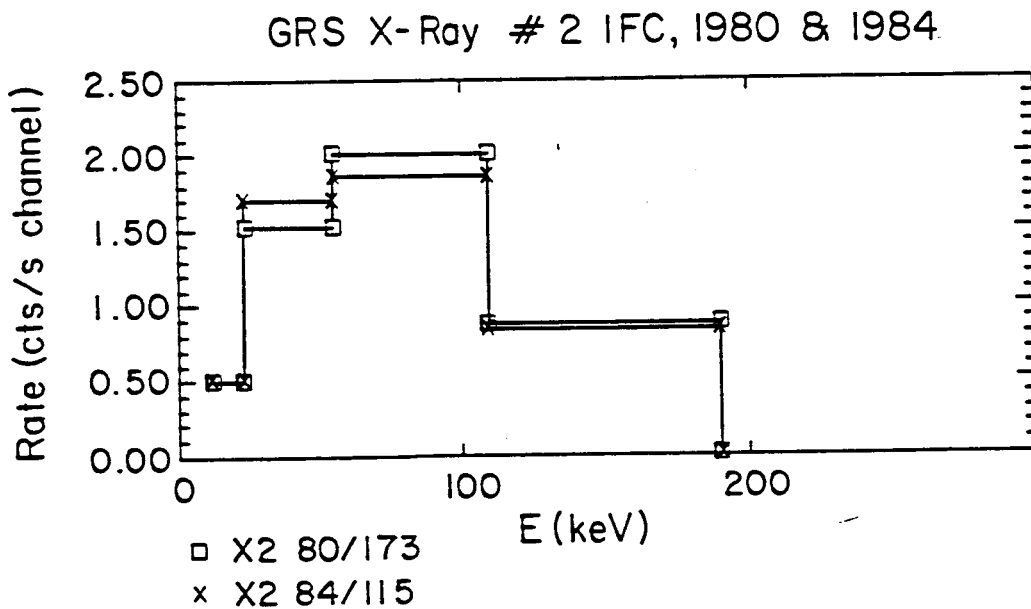
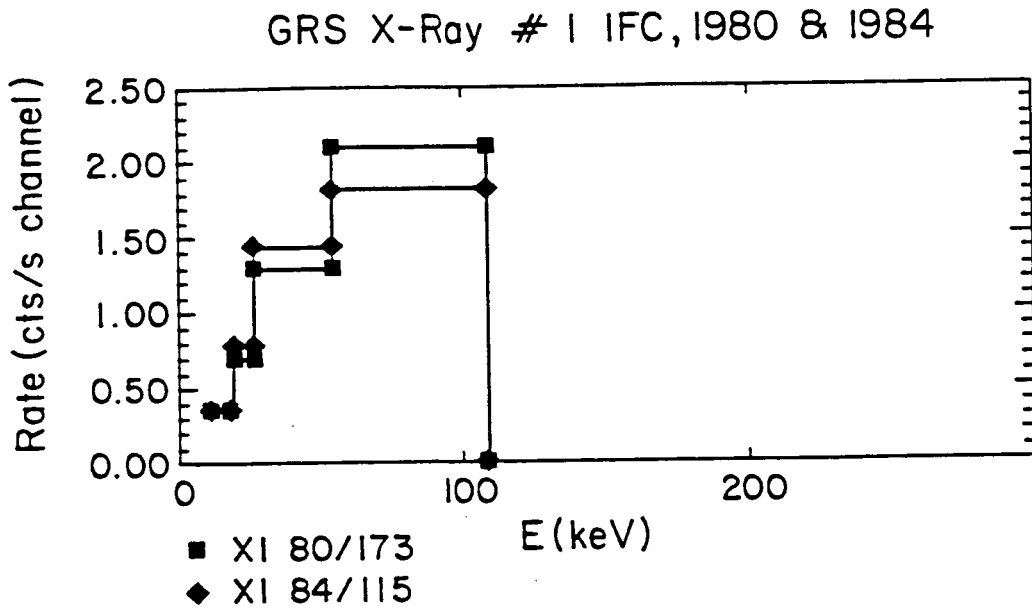


Figure 2 GRS inflight calibration in the X-ray detectors #1 and #2 on days of the year 173/1980 and 115/1984 respectively.

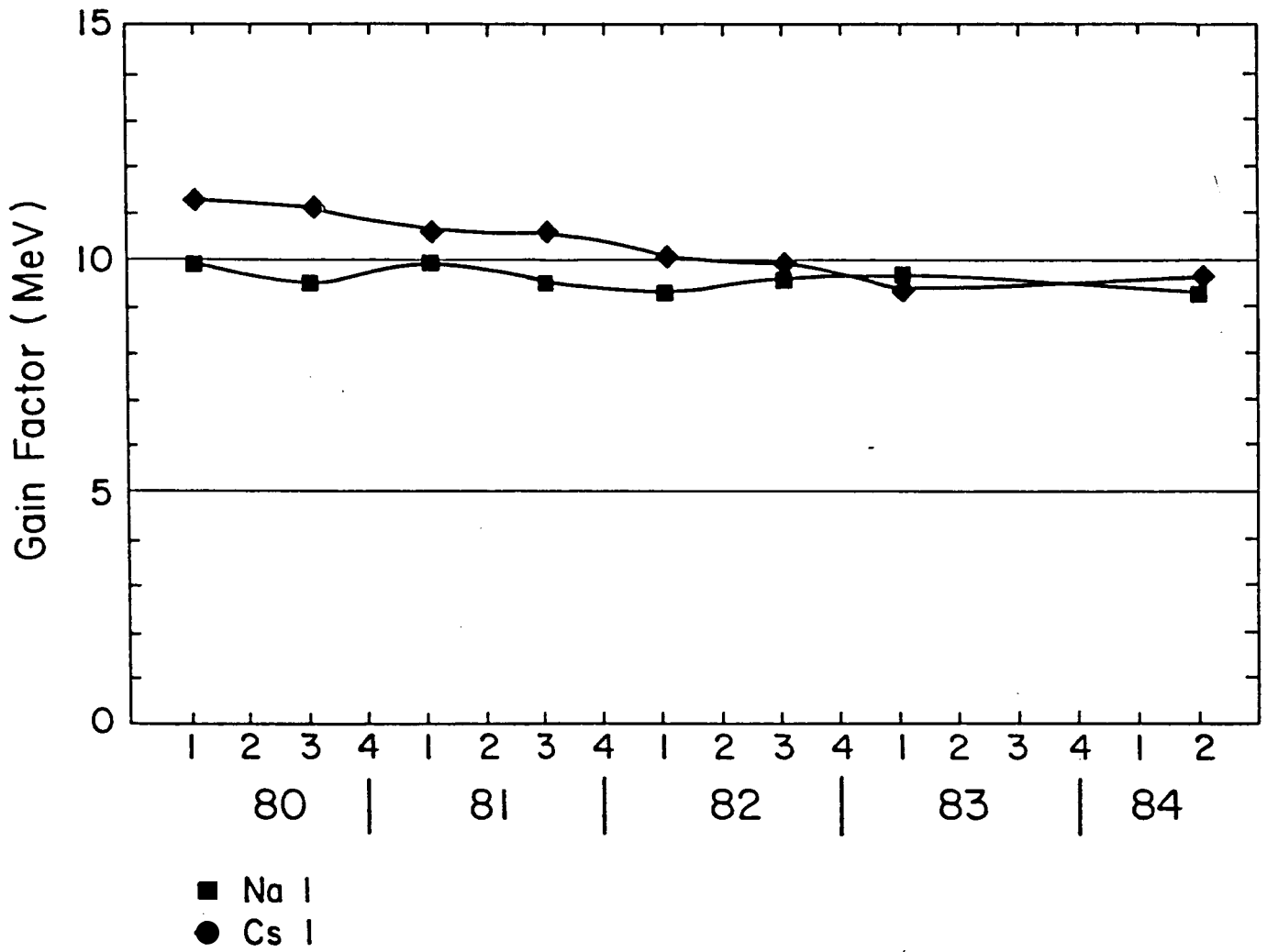


Figure 3 GRS high-energy monitor (HEM) inflight calibration gain factor from launch, 1980 February 14 to 1984 April 24.

any sensitivity changes and indication of less than 10% change in the HEMs gain over this 4-year interval. The stability of the main channel spectrometer (MCS) is illustrated in Figure 4, which shows the recorded spectra from the onboard ^{60}Co ($T_{1/2} = 5.3$ yrs). The decrease in peak intensity is due to the decay of the ^{60}Co calibration source. Significantly, the peak positions have changed less than 0.1%. As a final proof of the MCSs long-term stability, we show in Figure 5 the observed selected background spectra accumulated over a 3-year interval and containing over 1 year (i.e. 3×10^7 s) of integrated data. This long period stability in the three independent energy bands is allowing unprecedented flare comparisons.

3. BRIEF SUMMARY OF MAJOR RESULTS

3.1. SOLAR BURSTS

3.1.1. TIMING STUDIES

Prior to SMM only a handful of solar flares had been observed in the gamma-ray region. Based on these early data, the consensus was that flare acceleration took place in two phases. The first phase was thought to accelerate electrons to energies of ~ 100 keV in about 1 s. The second phase, which was thought to occur only in large flares, was thought to be the Fermi acceleration of ions and electrons to very high energies on a timescale of minutes.

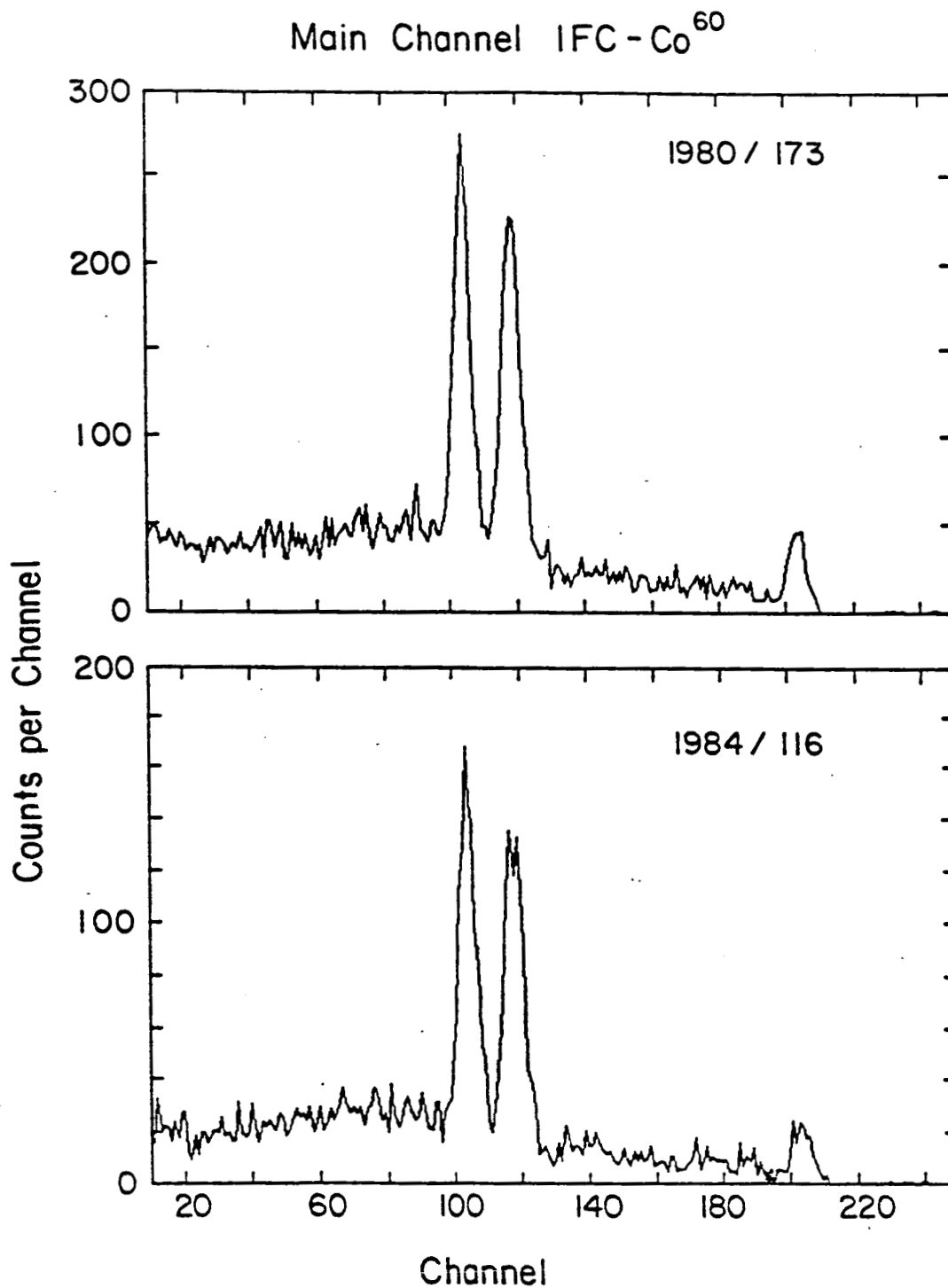


Figure 4. Main channel gamma-ray spectrometer inflight calibration ⁶⁰Co pulse height spectra for days of year 173/1980 and 116/1984 respectively.

SMM GRS
3 Year Accumulation
30,000,000 s

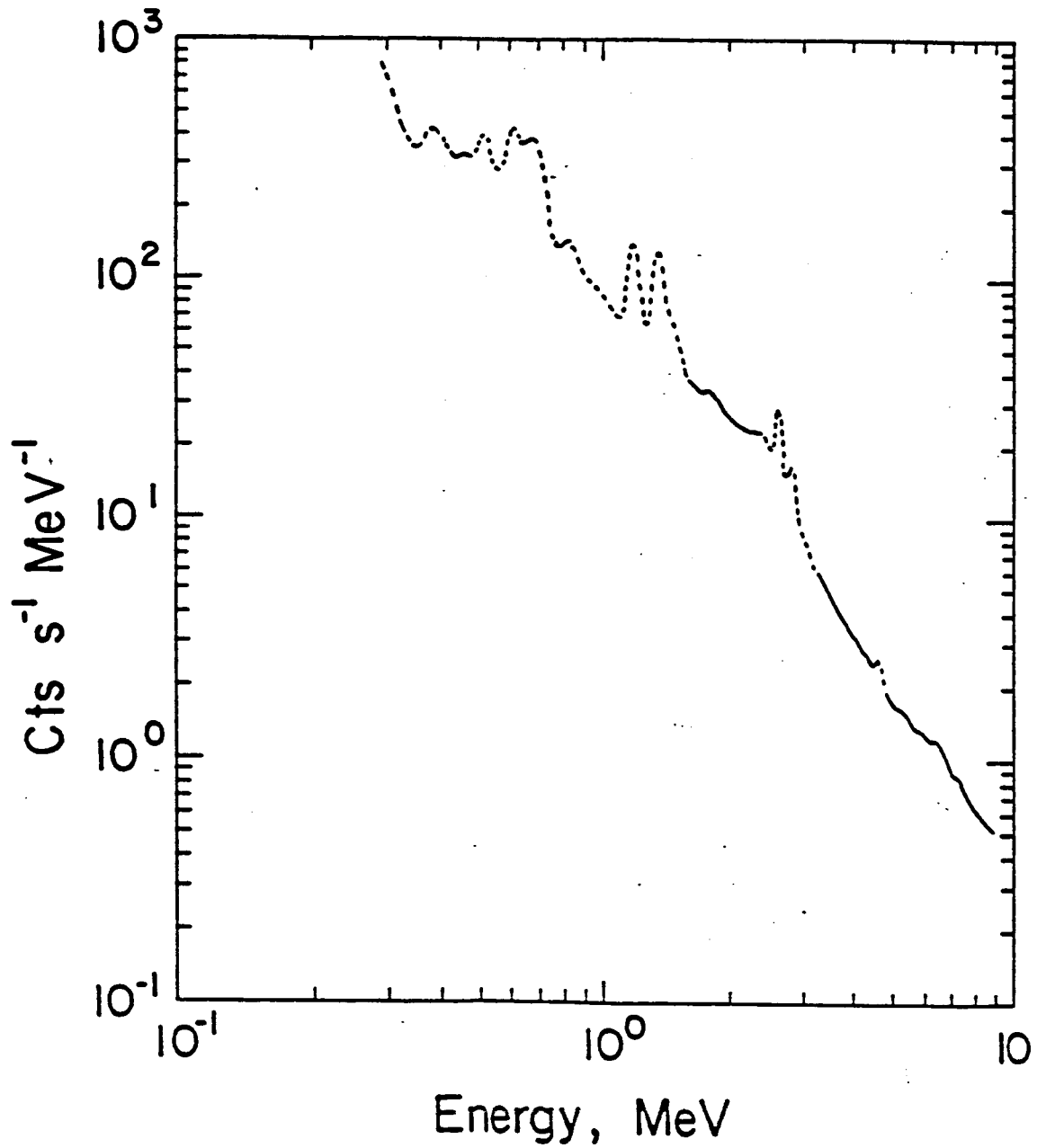


Figure 5. Main channel background spectra accumulated over a 3-year interval.

The data from the gamma-ray experiment on SMM have altered this view. These data conclusively show that both protons and electrons can be simultaneously accelerated to very high energies within a few seconds. This acceleration is often repeated several times during a flare, giving rise to distinct pulses of X-rays and gamma-rays. In addition, high-energy proton acceleration is much more common than previously thought and occurs in both large and small flares. Indeed, our data are consistent with the hypothesis that very energetic ions and electrons are accelerated in all flares.

The GRS gamma-ray observations show that the range of event durations runs from ~ 10 s to over 20 minutes. Most events include several emission pulses, which can be as short as 10 s in an event of ~ 1 minute duration or as long as ~ 2 minutes in an event of 20-minute duration (see Figure 6) (Forrest 1983). The shortest pulses are similar to the reported "elementary flare bursts" (EFBs) in hard X-rays < 100 keV (De Jager 1978), with widths varying between $4_{\pm 1}$ s and $24_{\pm 5}$ s for different flares. At lower photon energies (< 270 keV), structure is observed on timescales as short as 0.1 s (Hurley et al. 1983; Kiplinger 1983). In a preliminary study of several GRS events (Gardner et al. 1981), it was found that the time of the maximum count rate in an individual burst in the 4.1-6.4 MeV energy band, occurred between 2 and 45 s later than the corresponding maximum for the hard X-rays > 270 keV. The retardation of the pulse seems to be proportional to the pulse rise time.

However, simultaneous peaking of low-energy (< 100 keV) and high-energy (> 10 MeV) photons is also observed, limited only by the GRS

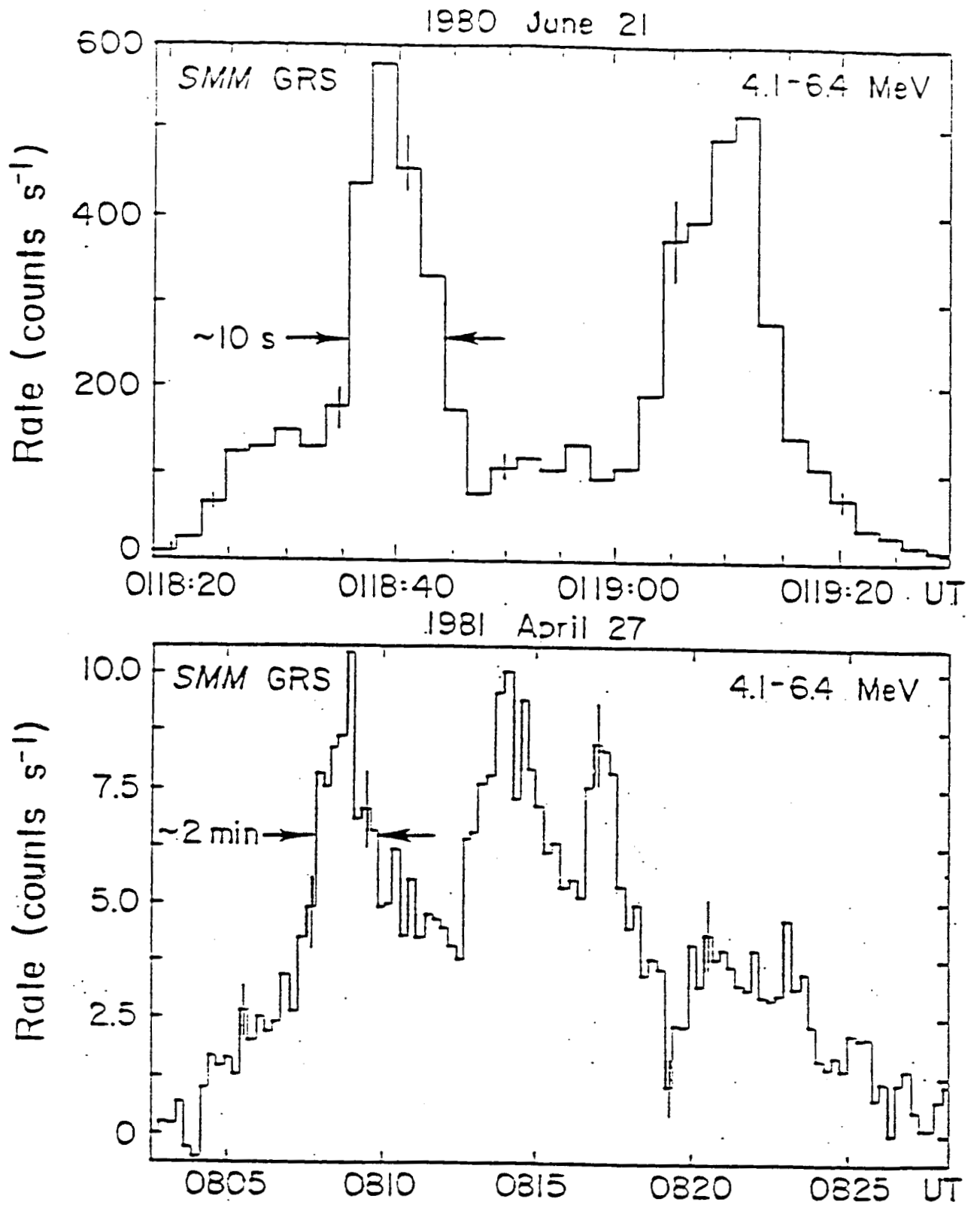


Figure 6.

A comparison of the extremes of duration, the rise time, and the burst width for two impulsive flares in gamma-ray emission at 4.1-6.4 MeV (from Forrest 1983).

time resolution. Figure 7 shows the count rates for a flare with several pulses of photons extending from 40 keV to 25 MeV; all occurring within a time interval of ~ 2 minutes. At ~ 1249 UT photons having energies < 300 keV were strongly attenuated by the atmosphere, since SMM was just entering sunlight. The peak intensities for the third impulse at ~ 1250 UT occur simultaneously at all photon energies to within ± 1 s. This means that the particles producing the energetic photon emission up to > 25 MeV were injected into and interacted with the target medium at the same time ≤ 1 s (Kane et al. 1986).

The earliest time at which photon emission is present at different energies in a flare has been determined in two intense bursts (Forrest and Chupp 1983), by comparing the starting times in several energy bands from ~ 40 keV to 6.4 MeV. Event initiation in each band was simultaneous to within ± 0.8 s in one flare and ± 2.2 s for the other. Again, this close timing over such a wide energy range requires that all energetic particles be interacting in the target at the same time. In the same events, the time of the peak intensity at the higher photon energies (> 4 MeV) was characteristically later (≥ 2 s) (Forrest and Chupp 1983; Nakajima et al. 1983). A similar temporal pattern was observed in over 40 flares with emission > 300 keV by the Hinotori satellite (Yoshimori et al. 1983).

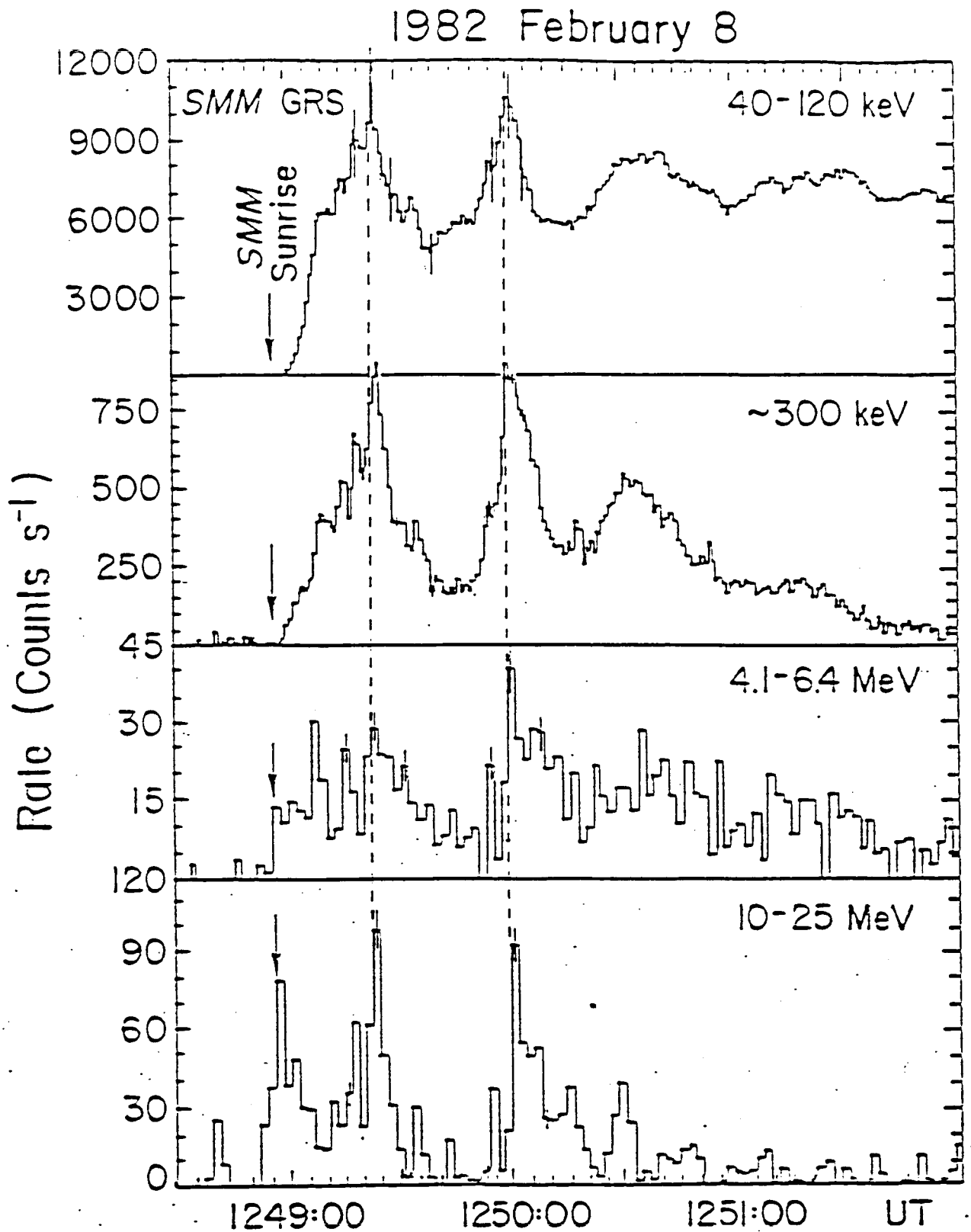


Figure 7.

The time history of photon emissions from 40 keV to ~ 25 MeV is shown for the flare on 1982 February 8, which occurred before 1249 UT. Early in the flare, low-energy photons $\gtrsim 300$ keV are occulted by the Earth's atmosphere. The times of the peak intensity for the pulse at ~ 1250 UT are the same within 2 s for all photon energies.

3.1.2. NARROW NUCLEAR LINES

Energetic ions generated during solar flares can interact with thermal ions in the solar atmosphere and produce gamma-ray lines. To illustrate, we show in Figure 8 the net count spectrum for the impulsive phase of a flare in which gamma-ray lines are clearly present. This spectrum is obtained after removal of primary electron bremsstrahlung continuum. The gamma-ray lines are due to ion interactions.

Individual nuclear gamma-ray lines have been detected in a number of the strong flares observed by the SMM GRS. Features have been identified with nuclei ranging from ${}^7\text{Li}$ to ${}^{56}\text{Fe}$. When compared with the theoretical synthetic spectra of Ramaty et al. (1979), the relative strengths of these features allow one to determine the composition and the energy spectrum of accelerated ions as well as the composition of the solar atmosphere. One of the exciting results derived from the GRS data is that the relative abundance of elements in the interaction region differ significantly from standard photospheric abundances. (Murphy et al. 1985)

To date, the relative strengths of lines has only been studied for a few limb flares. In the future we plan to study a number of other flares, including a few located on the solar disk. At the same time we will attempt to identify some of the statistically significant but unidentified features in the GRS spectra.

The study of line strengths will also be accompanied by a study of line widths and Doppler shifts. The incident particle that excites the nucleus

1981 April 27

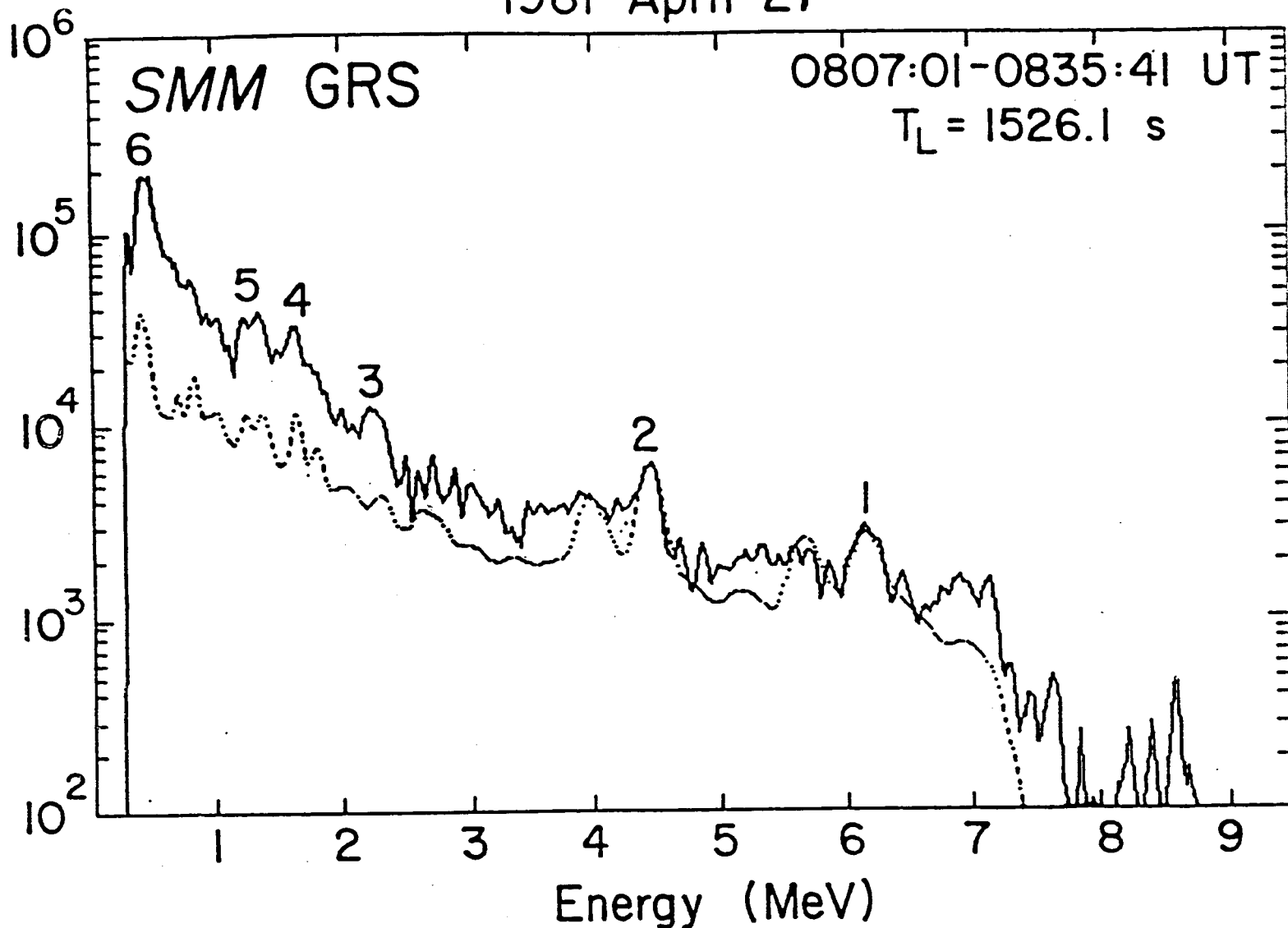


Figure 8 .

The time-integrated excess γ -ray counts spectrum above background (solid curve), after removal of a bremsstrahlung continuum, is shown for the 1981 April 27 flare (Forrest et al. 1983). Significant gamma-ray line features and their origin are (1) 6.129 MeV (^{16}O); (2) 4.439 MeV (^{12}C); (3) 2.313 MeV (^{14}N) and 2.223 MeV (ny); (4) 1.634 MeV (^{20}Ne); (5) 1.369 MeV (^{24}Mg) and 1.238 MeV (^{56}Fe); and (6) 511 keV (β^+), 478 keV (^7Li), and 431 keV (^7Be). The 2.223-MeV line, normally the strongest for disk flares, is strongly suppressed in this limb flare. The dotted curve is based on a predicted incident photon spectrum folded through the instrument response. The incident spectrum was generated assuming an accelerated ion spectrum of the form $\alpha T = 0.02$, incident on an ambient thick target with "standard" photospheric abundances (Ramaty et al. 1983).

can also impart a substantial kinetic energy to it. If the excited nuclear level emits a line photon on a timescale that is short when compared to the stopping time for the nucleus, the deexcitation photon will be Doppler shifted. The width of the deexcitation line can therefore provide clues about the energy spectrum of the incident particles. Furthermore, any anisotropy in the incident particle distribution can shift the centroid of the line. Ramaty and Crannell (1976) have shown that a Doppler shift as large as 40 keV is possible for the ^{16}O line at 6.1 MeV. A study of line widths and Dopplers shift can therefore provide clues about the energy spectrum of ions as well as their angular distribution.

3.1.3. BROAD BAND NUCLEAR EMISSION

Since nuclear lines may be significantly broadened and shifted, we have also developed a broad-band technique for measuring the nuclear component in flares. The bremsstrahlung and nuclear components are separated by assuming that essentially all of the emission below 1 MeV is electron bremsstrahlung and is described by a power law. The power-law photon spectrum is then folded through the instrument response function and fitted to the count spectrum below 1 MeV. The excess above this fit in the energy range 4-8 MeV, a region known to be rich in nuclear line emission, is a good measure of the nuclear component.

The GRS data indicate a good correlation between the 4-8 MeV excess and the fluence of X rays > 270 keV from electron bremsstrahlung (Forrest et al. 1983). This correlation is illustrated in Figure 9. The instrument

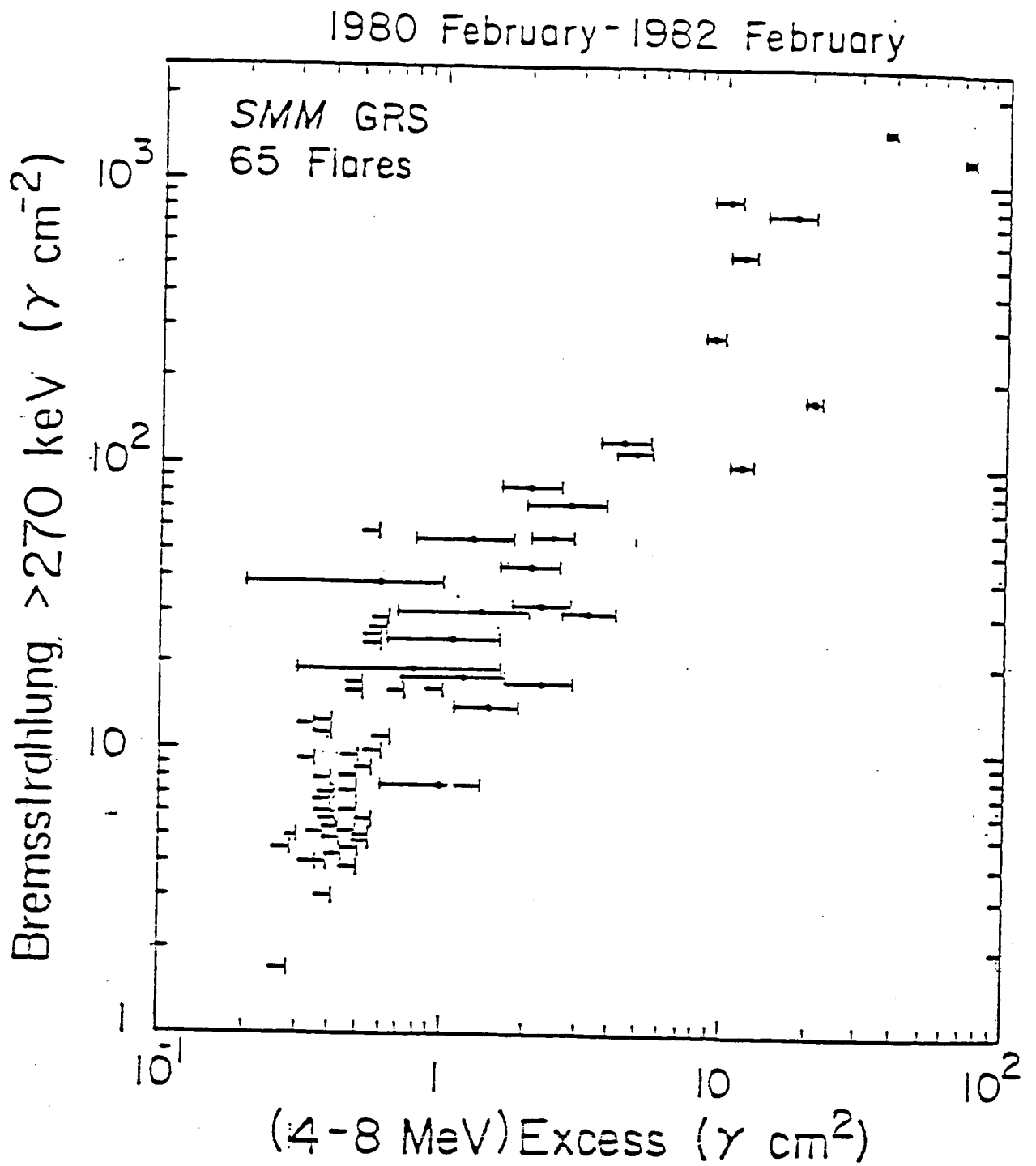


Figure 9.

The fluence (total time-integrated flux) of γ -ray > 270 keV is compared with the 4-8 MeV excess for GRS events observed between 1980 February and 1982 February (from Forrest 1983).

sensitivity limit for the (4-8) MeV fluence is 1 photon cm^{-2} . Down to this level the bremsstrahlung fluence is well correlated with the (4-8) MeV excess.

Our preliminary conclusion is that electron acceleration in flares is always accompanied by ion acceleration. This conclusion is at odds with the earlier idea that energetic ion acceleration is uncommon. We intend to refine this study in the future by using improved model spectra to more clearly separate the bremsstrahlung component from the nuclear component.

We recently initiated a search for nuclear emission from relatively large X-ray flares that were not detected at 300 keV. If our failure to detect these events at 300 keV is due to directivity of the bremsstrahlung radiation then it may be possible to detect nuclear emission from these events. We plan to make a systematic search for nuclear emission from these strong disk events.

3.1.4. NEUTRON CAPTURE LINE

The strongest gamma-ray line in solar flare spectra is the 2.22 MeV line produced when thermal protons capture neutrons to form deuterium (Ramaty et al. 1975; Chupp 1983). The process responsible for production of the prompt nuclear deexcitation lines, the interaction of flare accelerated ions with the solar atmosphere, also generates energetic neutrons. These energetic neutrons subsequently thermalize and are captured by photospheric protons on a timescale of 100 s. Compton scattering substantially

attenuates this line in flares at heliocentric angles $\theta > 85^\circ$. However, the delayed nature of the neutron capture line and the absence of background lines at 2.22 MeV, make the 2.22 MeV line relatively easy to measure in many of our strong flares.

A search for the neutron capture line in energetic flares observed by GRS from 1980 to 1983 has been initiated. Forty percent of 81 flares detected flux above 350 keV had detectable 2.223 MeV line emission (Share et al. 1985b). Our studies of the SMM GRS measurements indicate that the 2.22 MeV line fluence is well correlated with the (4-8) MeV excess fluence. This suggests, in agreement with theoretical calculations (Wang and Ramaty 1974; Ramaty et al. 1975), that the 2.22 MeV line fluence is a good measure of the energetic ion component in a flare. The intensity of the emission is also well correlated with the 40-140 keV hard X-ray intensity. There is no evidence for a size threshold for production of the line. These observations, together with the broad-band nuclear studies discussed above, suggest that ion acceleration in flares is a common occurrence.

We have made a preliminary study of the correlation between 2.22 MeV line fluence and the X-ray fluence rate in the (40-140) keV band. This correlation seems to indicate that ion acceleration is not only common in flares but that the ratio of the number of energetic electrons to energetic ions is fairly constant from flare-to-flare.

We plan to continue our studies of the time dependence of the 2.22 MeV line (Prince et al. 1984). The free neutron lifetime in the photosphere can be

determined by comparing the time dependence of the 2.22 MeV line with that of nuclear deexcitation lines. The neutron removal timescale depends on the relative abundance of ^3He and ^1H as well as the thermalization timescale (Wang and Ramaty 1974). The time dependence of 2.22 MeV line can therefore measure the abundance of ^3He in the photosphere.

Finally, we initiated a search for "quiescent" 2.22 MeV line emission from the Sun. By accumulating spectra for periods when flares were not detected by SMM GRS, we hope to detect or place a stronger limit on quiescent neutron production. Such a measurement is interesting because it can place a limit on the fluence from flares below the threshold of SMM GRS as well as address the question of whether or not ions are continuously accelerated and stored in coronal magnetic fields (see e.g. Elliot 1973). This measurement could also be used to constrain the tritium production rate in the solar atmosphere which may be useful for comparison with solar wind measurements.

3.1.5. POSITRON ANNIHILATION LINE

The positron annihilation line at 511 keV is another feature that has been detected in a number of flares by SMM GRS. The positrons are the decay products of positively charged pions and radioactive nuclei that are generated by the interaction of flare accelerated ions with the solar atmosphere. Unfortunately, the line is difficult to analyze because of a strong, highly variable background line at the same energy.

Nevertheless, SMM GRS observations of the 511 keV line have been studied for the two intense flares, 1980 June 21 and 1982 June 3 (Share et al. 1983). These studies already allow us to place constraints on the annihilation region. In both flares the line width is < 20 keV. This constrains the temperature in the annihilation region to less than 3×10^6 K. The line intensity decay profile in the 1980 June 21 flare is consistent with the profile expected for positrons that are generated by the decay of radioactive nuclei and are slowed down in a region with number density $> 10^{12}$ cm $^{-3}$. The line history for the 1982 June 3 flare shows the same general trend. However, it shows some deviations that can be interpreted as evidence for positrons from pion decay. This interpretation requires a density in the interaction region of $> 10^{14}$ cm $^{-3}$.

3.1.6. HIGH-ENERGY GAMMA-RAY AND NEUTRON EMISSION

The most energetic neutral quanta expected from solar flares are bremsstrahlung gamma-rays from primary and secondary electrons, π^0 decay gamma-rays, and neutrons (>50 MeV).

High-energy neutrons have been unambiguously detected from two large flares by SMM GRS. We briefly review those observations here. The first flare to provide evidence for energetic neutrons was the flare at 01:18:20 UT on 1980 June 21 (Chupp et al. 1982; Ramaty et al. 1983). The observations show strong emission at energies >10 MeV in a 65 s impulsive phase, followed by a low-intensity excess lasting at least 1000 seconds (see Figure 10a). Figure 10a shows the photon spectrum measured during the impulsive phase of

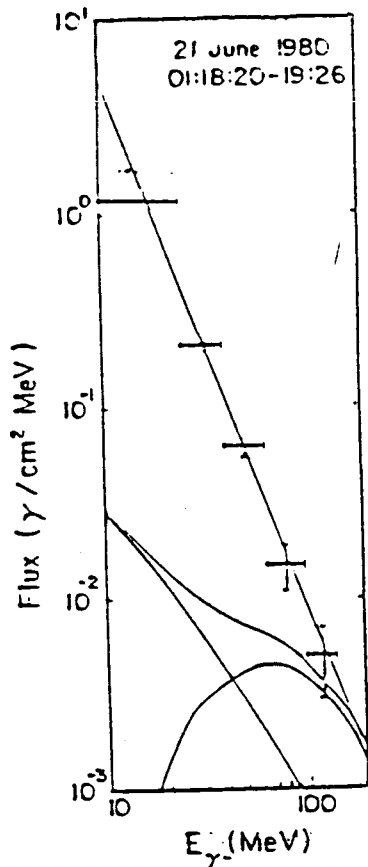


Fig. 10a.. The (10-140) MeV photon spectrum for the impulsive phase of the 1980 June 21 flare.

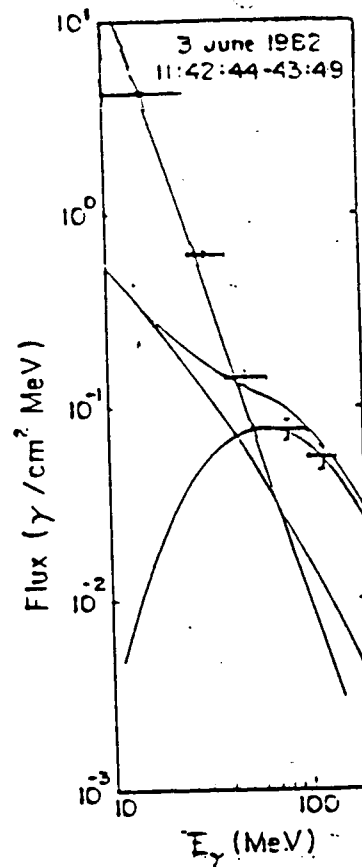


Fig. 10b. The (10-140) MeV photon spectrum for the impulsive phase of the 1982 June 21 flare.

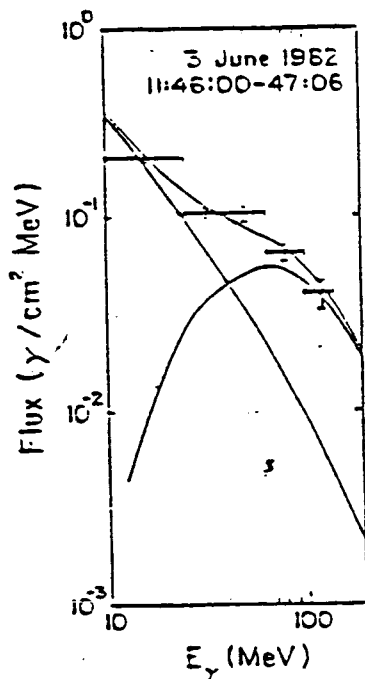


Fig. 10c. The (10-140) MeV photon spectrum early in the extended phase of the 1982 June 3 flare.

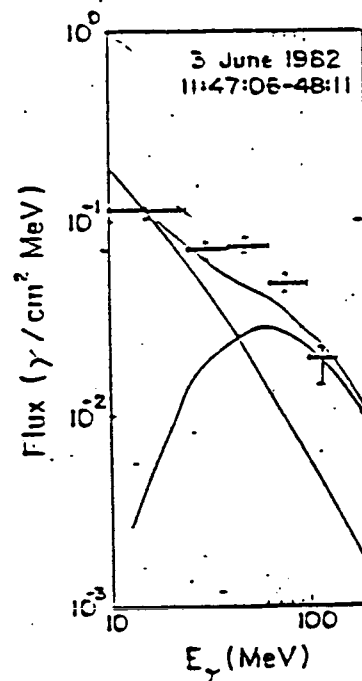


Fig. 10d. The (10-140) MeV spectrum showing the photon spectrum and the effects of the high-energy neutrons in the extended phase of the 1982 June 3 flare.

this flare. The solid curves in this figure are the best-fit photon spectrum, determined by combining both bremsstrahlung and pion decay spectra. The power-law spectrum is $(5.0 \pm 0.1) (E/10 \text{ MeV})^{(2.7 \pm 0.1)}$ photons $\text{MeV}^{-1} \text{ cm}^{-2}$ and the integral of the neutral pion spectrum is $0.6 \text{ photons cm}^{-2}$. The statistical test used to determine these values shows that while the overall fit is better with the pion spectra, the improvement is not sufficiently large to require it. Hence, the above pion flux must be considered an upper limit. Note however, that the data do require photons with energies $>100 \text{ MeV}$. In the extended phase we find that neither the spectral properties nor the observed ratio of "mixed" to CsI counts (Chupp et al. 1985) is consistent with a signal composed entirely of gamma-rays. We find that only $13 \pm 6\%$ of the observed counts during this period can be due to photons. The corresponding upper limit on the neutral pion photon flux is $0.5 \pm 0.2 \text{ cm}^{-2}$.

The time histories for the flare of 1982 June 3 are shown in Figure 10b-d. Again the high-energy observations show strong emission in an impulsive phase. However, in this event the impulsive phase is followed by a more intense extended phase. Figure 10b shows the photon spectrum observed during the impulsive phase. Again, these data indicate an intense power-law continuum component. However, in this case the data show a strong hardening at energies $>40 \text{ MeV}$. The best explanation of this hard component seems to be a neutral pion photon spectrum with a integrated flux of $12 \text{ photons cm}^{-2}$. Figure 10c shows a spectrum from the beginning of the extended phase. The data in this interval can be fit with a combined

charged and neutral pion photon spectra. In this case the required charged-to-neutral pion ratio is 3.1 ± 0.2 .

Finally, in Figure 10d we show a spectrum taken later in the extended phase. In this case the data was fit under the assumption that all the counts are due to photons. The data in Figure 10d show that secondary electron bremsstrahlung and pion decay emission can provide a good fit in the lowest and the highest channels. However, the observations exceed the model predictions in the three middle channels. Both the spectral shape and the time dependence of this excess is comparable to what is expected from high-energy neutrons. Chupp et al. (1985) have used these clues to study high-energy neutron production in this flare.

As a confirmation of the pion intensities deduced from gamma-ray spectral shape arguments, we note that these intensities are a predictor of the 511 keV line flux from charged pions. As an example we use the spectrum shown in Figure 10c, which requires an integrated neutral pion decay flux of $7.8 \pm 0.4 \text{ cm}^{-2}$. With our observed charged-to-neutral pion ratio of 3.1 ± 1 , and a positive-to-total charged pion ratio of 0.70, our predicted 511 keV flux is $0.12 \pm 0.02 [f(0.511)] \text{ photons cm}^{-2} \text{ s}^{-1}$. Here, $f(0.511)$ is the 0.511-to-positron ratio (Murphy and Ramaty 1985). Share et al. (1983) found that the total flux during this period was $0.35 \pm 0.05 \text{ photons cm}^{-2} \text{ s}^{-1}$. Murphy and Ramaty (1985) found that only $\sim 0.15 \text{ photons cm}^{-2} \text{ s}^{-1}$ could be accounted for by the radioactive positron emitters produced mainly in the impulsive phase. The difference between the measured value and Murphy's

values is $0.20 \text{ photons cm}^{-2} \text{ s}^{-1}$, which is in agreement with our predictions for charged pions if $f(0.511) \sim 1.5$.

The highest energies attained by ions during flares can be determined by direct observation of neutrons at the Earth (Chupp et al. 1982; Chupp et al. 1984; Debrunner et al. 1984). The GRS has detected the characteristic signature (Lingenfelter and Ramaty 1967) for neutrons produced at the Sun in a time interval short compared with the neutrons' transit time to the Earth. (see Figure 11). The inset in the figure, shows the time profile of photon with energies $> 10 \text{ MeV}$. This profile reflects the production time history of energetic gamma-rays and neutrons at the Sun. The signal which peaks at $\sim 500 \text{ s}$, is probably due to neutrons (Chupp et al. 1982) with energies between 50 MeV and $\sim 500 \text{ MeV}$.

A second event with neutrons of energy $\sim 1 \text{ GeV}$ on 1982 June 3 has also been recorded by GRS (Chupp et al. 1984) and by ground-level neutron monitors (Debrunner 1984; Kocharov 1983). Neutron decay protons near the Earth in the same event have also been observed (Evenson et al. 1983). In this event, we find a time extended production of neutrons is required to account for the response of the GRS and the Jungfraujoeh neutron monitor throughout the delayed phase. Therefore a delta function production in the impulsive phase cannot account for the observations of the neutron monitors and the GRS to solar neutrons. As a consequence there is not a one to one correspondence of arrival time to neutron energy, and this complicates the determination of a neutron spectrum. Also, a neutron production spectrum resulting from a Bessel function flatter than $\Delta T = 0.05$ may be required to

1980 June 21

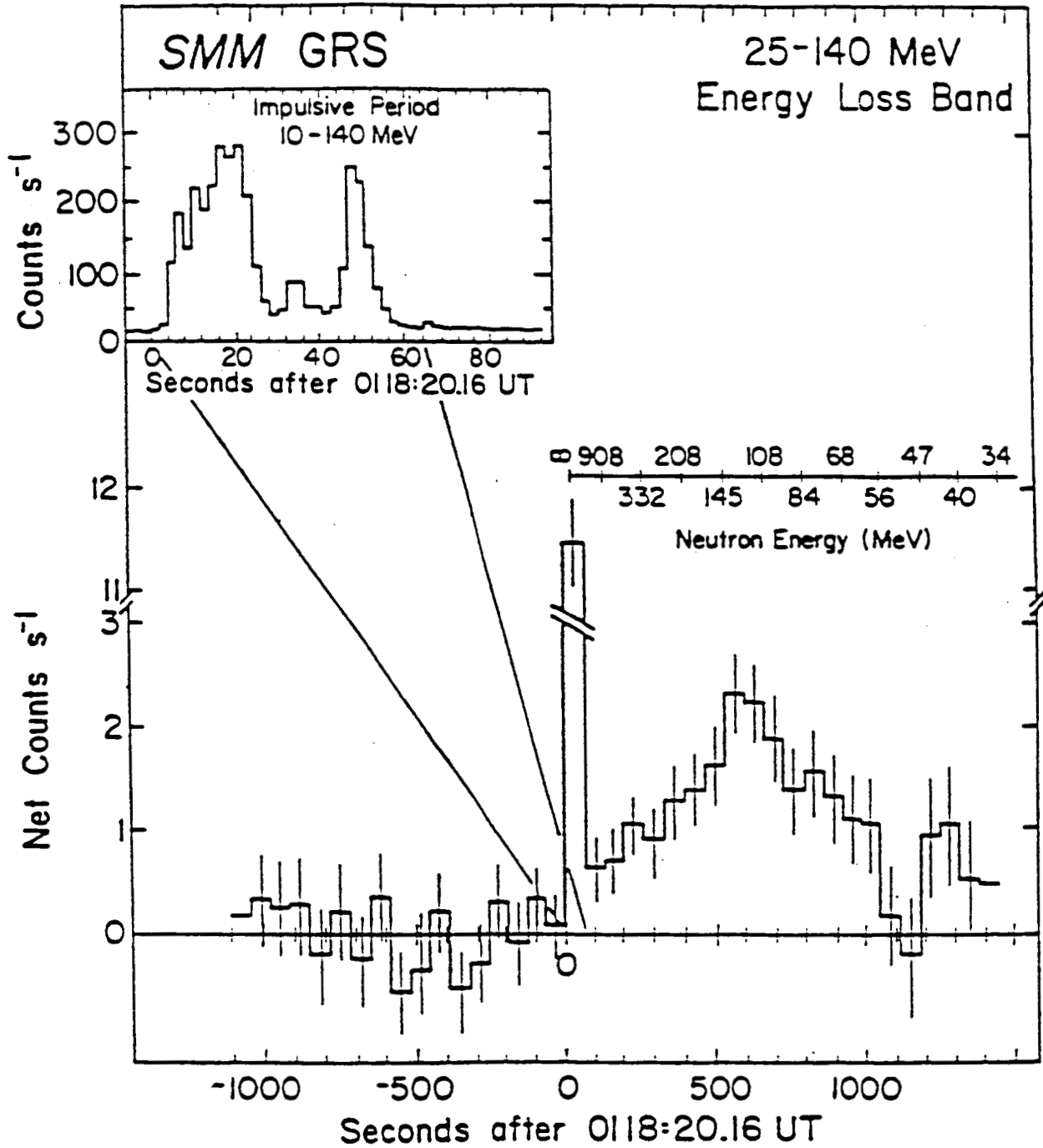


Figure 11. The arrival time history of energetic photons > 25 MeV and neutrons at the Earth is shown for the intense flare on 1980 June 21, as recorded by the GRS (Chupp et al. 1982)

pull the predicted neutron count ratio down to that required for the GRS simultaneous response to both neutrons and γ rays. As previously pointed out (Murphy and Ramaty 1985; Ramaty et al. 1983) a power-law spectral shape which is constant from 1 GeV down to 50 MeV does not seem to be viable.

Since GRS observations have established that impulsive photon emission from solar flares can extend to > 50 MeV and that neutrons can be produced with energies as high as 1 GeV, we conclude that either an extremely rapid particle accelerator is operative or that preaccelerated particles are released impulsively into a target. A comprehensive study of all events with high-energy emission is currently underway.

3.1.7. DIRECTIVITY OF THE CONTINUUM EMISSION

Anisotropies in the velocity vector distribution of flare-generated energetic electrons can provide important clues about particle acceleration and about the transport of electrons within flaring regions. The distribution of detected solar flares with position on the Sun can be used to assay the directivity of flare radiation. For example, the fraction of events with heliocentric angles, θ such that $\sin \theta > 0.9$ is a good directivity diagnostic that has the advantage of being relatively insensitive to the details of the flare latitude distribution (Vestrand 1983). Using this diagnostic in a study of flares detected at 300 keV, we found (Vestrand et al. 1986) that one can reject the hypothesis that the flare radiation pattern is isotropic or upwardly directed at the 99% confidence level (see Figure 12). The data are nominally fit by a Gaussian

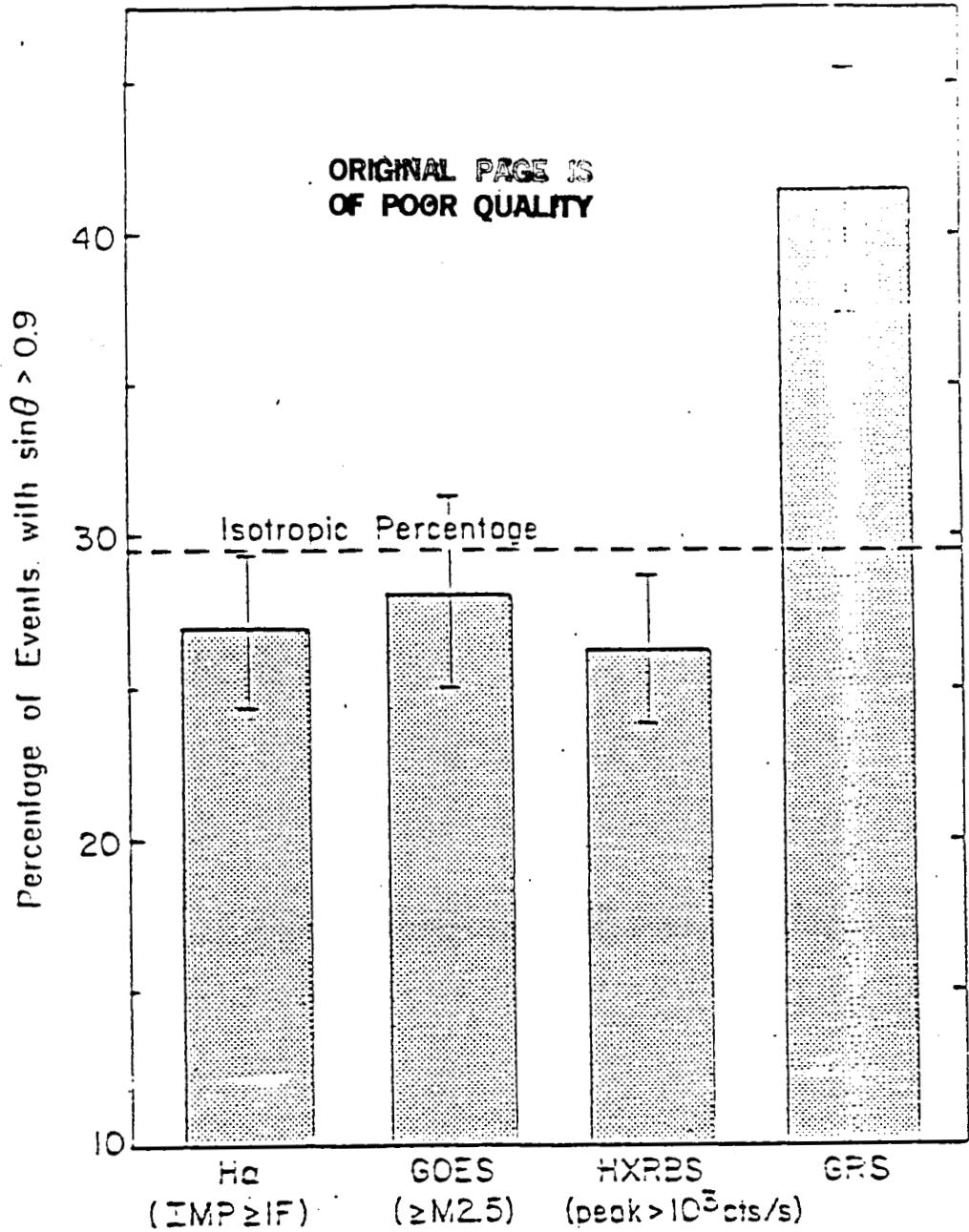


Figure 12. The percentage of limb events is shown for gamma-ray flares (GRS) detected between February 1980 and December 1982. Three control samples: GOES events, HXRBS events, and H α flares, are also illustrated. The control samples were selected from only that subset of the events that occurred when the GRS was capable of detecting a coincident event.

radiation pattern that is directed downward and has a half-power angle of $\phi_{1/2} = 90^\circ$.

Since Compton backscattering is relatively small at energies >300 keV, the directivity of the flare radiation must be generated by an anisotropy of the radiating electrons. Such an anisotropy will produce another potentially observable feature, namely, the spectra of the radiation should vary with viewing angle. Our statistical studies of the SMM GRS spectra indicate that a center-to-limb spectral variation is indeed present. If the spectra between 300 keV and 1 MeV are fit by power laws, we find that events near the limb tend to be harder than disk events by $\Delta S \sim 0.5$ (Vestrand et al. 1986). The simplest explanation of both the observed center-to-limb spectral variation and skewed position distribution is that the parent electron distribution is downwardly directed.

The observed enhancement of a number of events at the limb does not, of course, mean that more flares are actually occurring at the limb. Instead, the directivity of the radiation at 300 keV only makes it easier to detect smaller flares at the limb. If one makes the assumption that the intensity of a flare at energies where the radiation pattern is isotropic is a good indicator of the flare size, then one should find a number of disk flares that were not detected by SMM GRS that are just as large as those detected at the limb. A search for these events is currently underway.

3.1.8. EVIDENCE FOR PERIODICITY

One of the more intriguing findings of the SMM GRS experimenters is that flare activity has a 155 day period (Rieger et al. 1985). This is illustrated by Figure 13 which shows the occurrence times of flares that were detected at energies > 300 keV. While this discovery was initially discovered by analyzing the occurrence times of flares detected at high energies, subsequent work has shown that the periodicity is also present in the GOES soft X-ray (Rieger et al. 1985) and HXRBS hard x-ray (Kiplinger et al. 1985). The origin of this periodicity is unknown.

We have also examined the properties of flares to determine whether or not a particular class of events is responsible for the modulation. We find that the amplitude of the modulation is a strong function of flare size. For example, the amplitude for events with GOES size $> M 2.5$ is nearly twice as large as the amplitude for events with GOES size $> C1$. On the other hand, the number of potential flare sites (viz. sunspots or active regions) does not seem to be modulated. However, if one examines the number of active regions with relatively compact and complex magnetic topologies (magnetic classes BG, BGD, and GD) one finds a strong modulation. We are currently studying the implications of these findings.

3.1.9. COMPARISON OF GRS GAMMA RAYS WITH OTHER FLARE EMISSIONS

The first 2.5 years of GRS data were correlated with other flare observations, taking into account observation duty cycle, with the

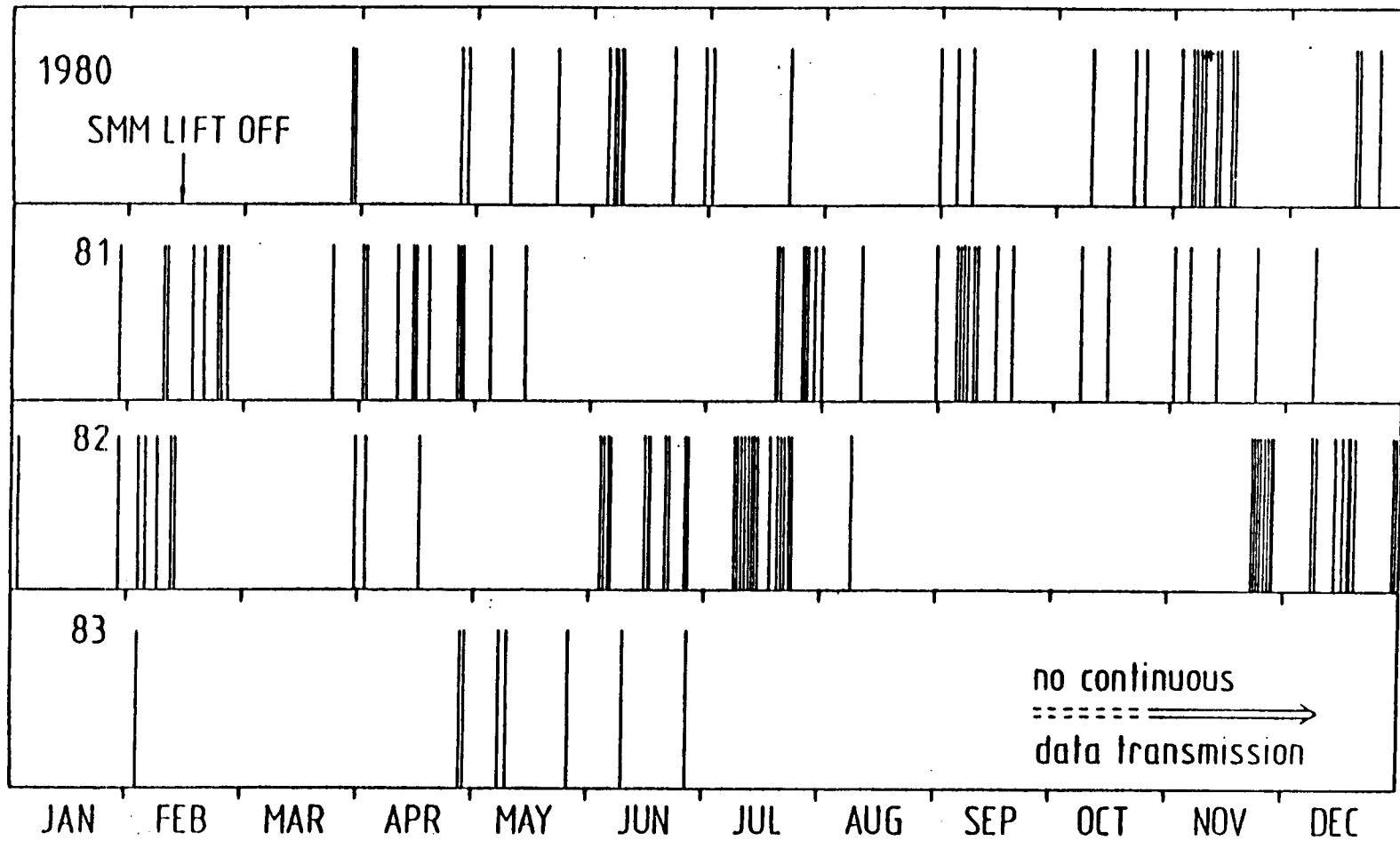


Figure 13. Energetic solar flare events with photon emission above 300 keV are illustrated by short vertical lines, plotted versus time for successive years of observation after the Gamma-Ray Spectrometer (GRS) began operation.

following results: (a) A gamma-ray event > 270 keV may be associated with any H α class, (b) 20% (10/50) of flares of class $\geq 2B$ have associated 4-8 MeV excess (Cliver et al. 1983), (c) 75% of all SMM GRS events > 270 keV are from H α of B (brilliant) class, (d) 50% (13/26) of GOES (1-8) A X-ray events with peak intensity $\geq X2$ have significant 4-8 MeV excess (Cliver et al. 1983), (e) GRS events > 270 keV are always associated with a solar microwave burst (≥ 1 GHz), and (f) 53% (19/36) of 9 GHz bursts with peak flux density ≥ 1200 FU have significant 4-8 MeV excess (Cliver et al 1983).

There is no correlation between the peak SEP* flux measured near the Earth and the GRS MeV excess fluence (Cliver et al. 1984). This lack of correlation is quite unexpected, since peak flux is a classic indicator of proton fluence injected into space (Van Hollebeke et al. 1979; Van Hollebeke, et al. 1975). This may indicate that the SEPs come from a different site or that they are produced by a different mechanism. The significance of the lack of correlation between SEP and gamma-ray events has been discussed in some detail (McGuire 1983). We note, however, that SEP flares with an enhanced flux ratio of electrons (6-11 MeV) to protons (24-44 MeV) generally have associated 4-8 MeV excess (Evenson et al. 1984; Evenson et al. 1983).

* We use solar energetic particles (SEPs) instead of the more common term solar cosmic rays.

We have also used observations by the SMM GRS to address the question: Are relativistic electrons accelerated in all flares? The detection of a flare at energies greater than 300 keV is good evidence for the presence of relativistic electrons. Using the peak thermal flux observed by the GOES satellites as a measure of flare size we find that the size threshold for detectability at >300 keV by SMM GRS is approximately GOES size M2.5. There is, however, a class of events that were not detected that occurred when SMM GRS was observing and had GOES sizes greater than M2.5. From the GOES properties alone there seems to be no parameter such as duration that distinguishes these events from those that were detected at high energies. However, the undetected events are preferentially associated with H alpha flares on the disk. We find the directivity of emission above 300 keV is probably responsible for the failure to detect these events. We have concluded that relativistic electrons are probably produced by all flares with GOES sizes greater than M2.5.

3.2. COSMIC GAMMA-RAY BURSTS

As well as measuring the gamma-ray properties of solar flares, the SMM GRS is continuing to make very interesting observations of cosmic gamma-ray bursts. Until recently, it was thought that 1 MeV emission would be weak in gamma-ray bursts. The rationale for this belief were the fact that several authors argued that the data at < 500 keV are best fit by thermal models which predict relatively little flux above 1 MeV and the fact that pair-production opacity could strongly attenuate > 1 MeV photons under the

physical conditions likely to be present at the burst sites. The discovery, by the SMM GRS experimenters, that strong emission at > 1 MeV is a common property of gamma-ray bursts has led to important changes in our ideas about the nature of cosmic bursts (Matz et al. 1985). The presence of this high-energy emission has ruled out several models and placed strict constraints on the physical conditions at the burst sites. The generation of this radiation has also become one of the central theoretical issues associated with gamma-ray bursts. The SMM GRS is currently the only instrument that is measuring > 1 MeV emission from cosmic bursts. Since more than 50% of the total energy in a burst can be carried by > 1 MeV photons, the continued monitoring of high-energy emission is essential for our understanding of gamma-ray bursts.

3.2.1. BROAD BAND SPECTRAL FITS

Broadband fits to spectra accumulated over 16 s have been made for bursts within the field of view of the instrument. For the most intense events a consistent picture is beginning to evolve. Most of these events have spectra which are too hard to be consistent with thermal emission models such as thermal bremsstrahlung or thermal synchrotron. In the weaker events it is difficult to discriminate between the models, but it is apparent that temperatures required to fit the thermal models may be too high to be physically realistic.

3.2.2. SEARCH FOR POSITRON ANNIHILATION FEATURES

A search has been conducted for evidence of Doppler shifted and broadened annihilation radiation in cosmic bursts. This search was performed on 22 events within the field-of-view of the instrument. To date we have found no statistically significant evidence for this line emission. These results seem to be at odds with the reported detections of the KONUS group. There was one event detected by both the KONUS and SMM instruments for which an extended emission feature at high energy was reported by the KONUS group (Mazets et al. 1981). However, no convincing evidence for an annihilation feature has been found in the SMM GRS data (Nolan et al. 1984). We plan to continue searching for possible annihilation features. We will place particular emphasis on those events that were also detected by the KONUS investigators.

3.2.3. HARDNESS RATIOS

For many years astrophysicists have attempted to discover a pattern in the spectral evolution of cosmic gamma-ray bursts. Recently the KONUS experimenters suggested that there is correlation between the luminosity and temperature in bursts, under the assumption that the emission is thermal bremsstrahlung. Data from both the GRS and HXRBS experiments on SMM conflict with this finding. In fact, evidence has been found for a pattern of hard-to-soft spectral evolution within resolved pulse structures in bursts. Figure 14 shows the spectral evolution for one of the bursts detected by the SMM GRS. This evolution may be a fundamental

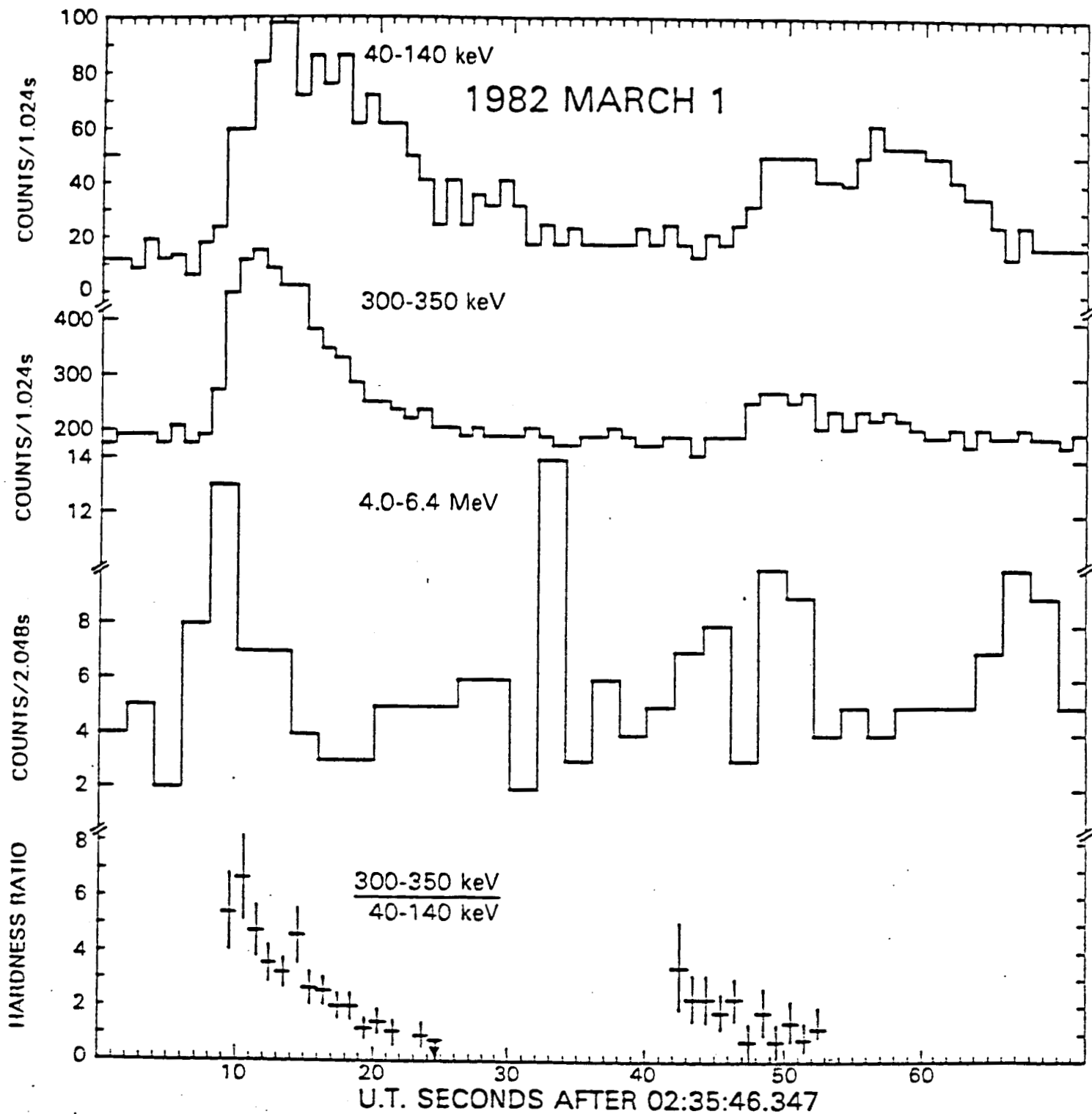


Figure 14. Time histories for the 1982 March 1 event. The time dependence of the hardness ratio is also illustrated (Norris et al. 1985)

characteristic of bursts. A study of this property by the SMM experimenters is in preparation.

3.2.4. SEARCH FOR LONGER DURATION EVENTS

A report of a 10 to 20 minute transient gamma-ray line event of unknown origin has appeared in the literature. This event was detected by a high resolution spectrometer experiment on board a balloon-borne spectrometer (Jacobson et al. 1978). Searches for such long duration line events have commenced using the GRS data. A preliminary search for a transient 2.223 MeV line covering a six-month period was not successful in locating such an event. We plan to enlarge the scope of this study by extending the search period. We also plan to add energy bands that cover other lines.

3.3. "STEADY" SOURCES

As part of the production processing of SMM GRS data, 3-day spectral accumulations have been derived. Three parameters which affect the instrumental background have been used to sort the spectral data: (1) time from the last anomaly passage, (2) zenith angle of the instrument; and (3) vertical cutoff rigidity. Each parameter is resolved into 10 elements. Therefore for each 3-day accumulation, 1000 spectra have been summed. Software has been developed to further analyze these data and has allowed detailed studies of the orbital background. With a better understanding of these backgrounds, it has become possible to use the SMM GRS data to study celestial gamma-ray line emission with high sensitivity.

Celestial line observations are possible because the detector's axis follows the Sun along the Ecliptic. The Galactic Center passes near the center of its field-of-view in the winter. Any source of detectable line radiation will therefore exhibit an annual modulation. Such a detection at high significance is discussed below in the section concerning detection of interstellar ^{26}Al line gamma radiation. Other studies are in progress.

3.3.1. GALACTIC ^{26}Al

The analysis of 3 1/2 years of data from the SMM GRS have shown a strong line radiation (Share et al. 1985a) near 1.81 MeV when the Galactic Center region traversed the instrument aperture (see Figure 15). All of our tests point to a galactic origin for the radiation. We have derived an energy spectrum by taking the difference between Galactic Center and Galactic Anticenter exposures. This difference spectrum shows the presence of single line in the 1.6 to 2.0 MeV region having an energy 1.804 ± 0.004 MeV and intrinsic width 38 ± 21 keV (FWHM). This is consistent with narrow line emission at 1.809 MeV from interstellar ^{26}Al . This is only the second confirmed nonsolar system gamma-ray line which has been observed and identified unambiguously.

3.3.2. GALACTIC POSITRON ANNIHILATION

One of the most exciting discoveries in gamma-ray astronomy has been the detection of variable source of annihilation radiation in the direction of the Galactic Center. The source was detected by balloon instruments and the HEAO-3 spectrometer. However, either late in 1979 or early in 1980, the

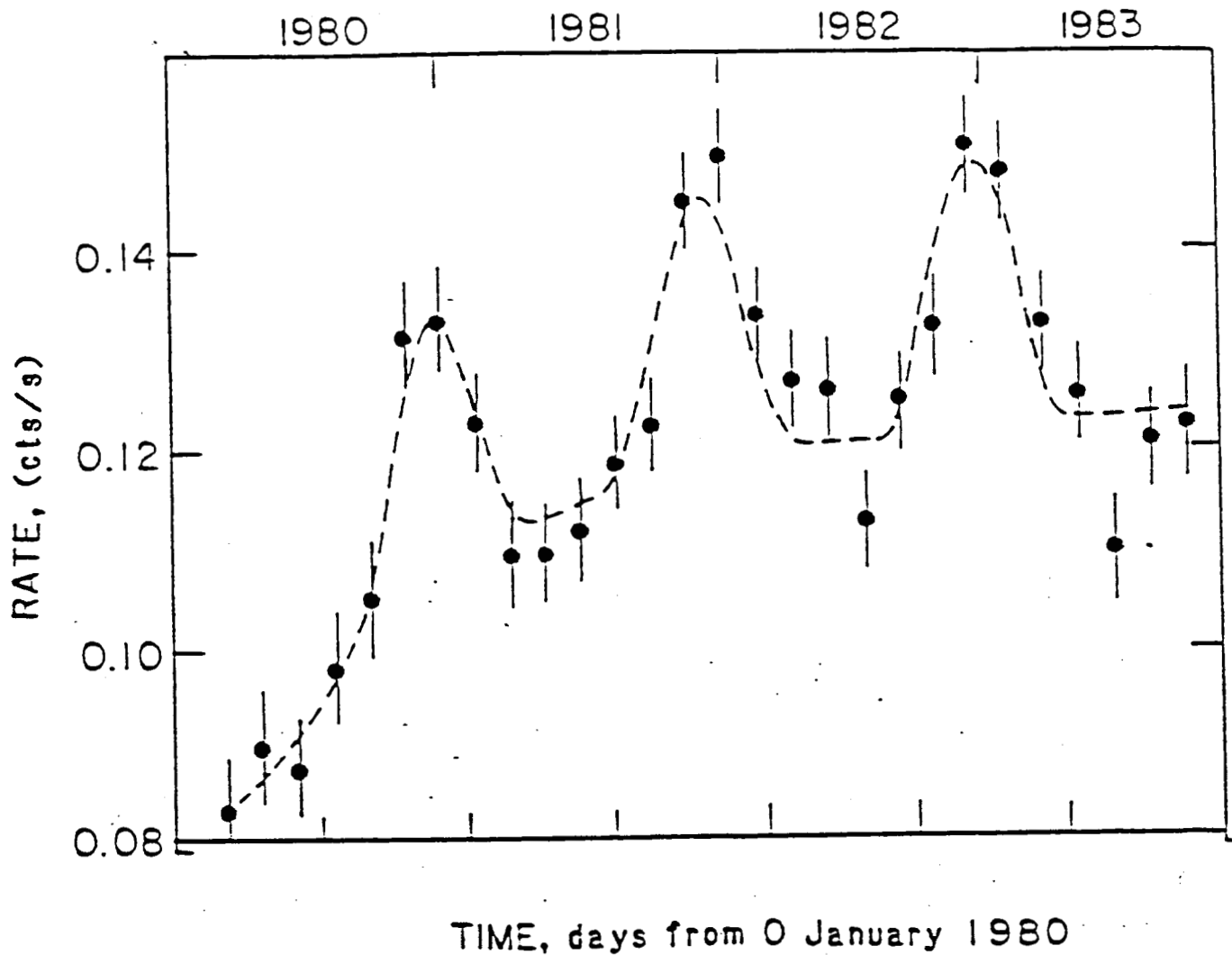


Figure 15. Variation in the intensity of a line at 1.81 MeV obtained when data from times $> 10,000$ s from the last SAA passage in the 1.6-2.0 MeV range are fit by a power-law continuum and lines at 1.75 and 1.81 MeV. The gradual increase in the 1.81 MeV intensity is due to the nearby ^{22}Na line which is not resolved in this two line fit. Sky-viewing data (zenith angle $< 72^\circ$).

source apparently decreased significantly in intensity. It has not been detected by subsequent experiments. An intensive effort has been underway to detect this annihilation radiation using the SMM data. Preliminary analysis indicates that the line should be detectable at the levels reported in the 1970's. In order to do so, systematic variations in the background 0.511 MeV must be well understood. After this analysis is completed we hope to set limits on the galactic center emission covering about 1/3 of each year that SMM continues to be in operation. These same observations may allow the instrument to detect a diffuse glow of 0.511 MeV line radiation from the Galactic Plane.

3.3.3. SEARCH FOR SPECIFIC TRANSIENTS

The GRS's large field-of-view makes it an ideal instrument for detecting transient cosmic events such as novae, nearby extragalactic supernovae, and other potential exotic objects, such as SS433. A study of SS433 using the SMM GRS has already been completed, (see below). Search of the data for other celestial transients is underway.

3.3.4. SS433

We have searched the SMM GRS data from 1980 to 1985 for evidence of the Doppler shifted nuclear lines from SS433 reported by the HEAO-3 group (Geldzahler et al. 1985). No evidence has been found for this emission in any of our spectra summed over 3, 9 and 360 days. Typical 99% confidence upper limits for 9-day summations are below the reported levels reported by

HEAO-3, while the 360-day limits are almost an order of magnitude below the constant level reported by HEAO-3 experimenters. Figure 16 shows a comparison of the HEAO-3 detections and the limits obtained using the SMM GRS.

In the coming year, we plan to systematically search our data base for a number of other potential sources. Targets, besides novae, include extragalactic supernovae, and exotic high-energy sources.

3.3.5. NOVAE

The possibility of a thermonuclear runaway occurring in association with novae (Starrfield et al. 1972) has led to predictions of detectable fluxes of gamma-ray lines from nearby (galactic) events (Clayton and Hoyle 1974; Truran 1975). Leventhal et al. (1974) have searched for the lines predicted (e.g. 1.275 MeV from ^{22}Na) during explosive nucleosynthesis several years after two novae and determined only upper limit fluxes. Prompt lines which could be detectable near the nova maximum are at 0.511 MeV and 2.31 MeV but have not been studied. Therefore, because of the long term SMM GRS data base we are initiating a search for transient gamma-ray line features during the early phases of galactic novae.

4. DATA PROCESSING AND ANALYSIS

4.1. OVERALL DATA PROCESSING RESPONSIBILITIES

The scientific and technical analysis of the GRS data is carried out by three separate research groups at UNH, MPE, and NRL. Each group has well

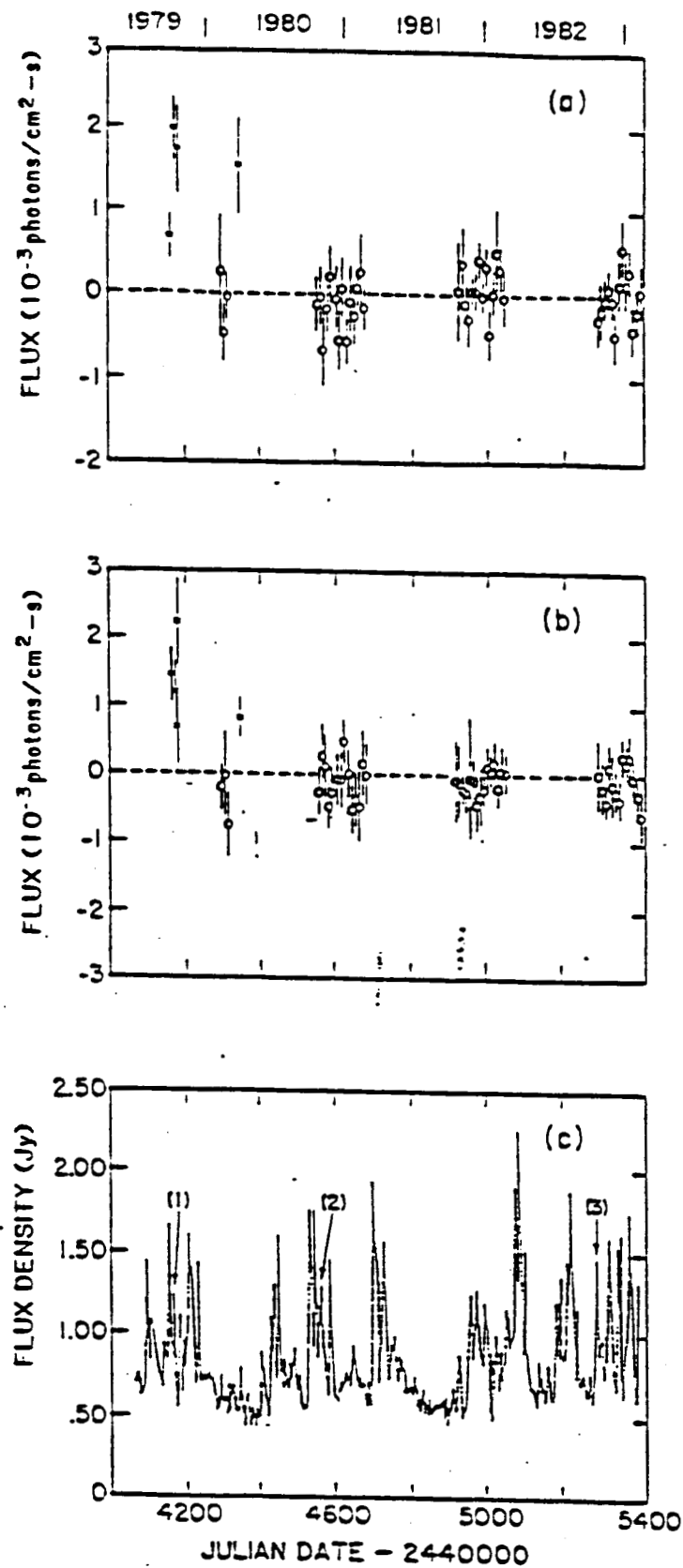


Figure 16. Light curves of the Doppler shifted ≈ 0.37 MeV gamma-ray line data from the SS433. HEAO-3 data (stars), SMM data (unfilled circles). a) blue beam, b) red beam. c) 2695 MHz radio light curve for SS433 (Geldzahler et al. 1985)

defined responsibilities. The UNH group had the pre-launch responsibility for instrument integration, testing, and calibration of the experiment at Goddard Space Flight Center. UNH also assumed responsibility, after launch, for instrument monitoring and for primary interaction with scientific groups responsible for the other instruments on SMM. This includes planning for short-term spacecraft operation. MPE and NRL have concentrated on software development.

One of the priorities of the GRS team has been the identification of flares which produced observable gamma-ray emission. The search for these gamma-ray events was carried out quasi-independently by all three groups. The resulting flare list, after confirmation by all three groups, is a list of ~ 500 flare events with detectable emission and a sublist of > 100 flares with a large enough signal to allow spectral studies. Some of the flare characteristics obtained from this list are discussed in Section 3.1. A current list of the solar events and cosmic events is available on request. A final listing will be included in catalogues in preparation under the follow-on grant.

In the following sections we outline our existing data analysis procedures and describe how these procedures have evolved as our analysis progressed.

4.2. UNH DATA ANALYSIS PROGRAM AND DOCUMENTATION PLANS

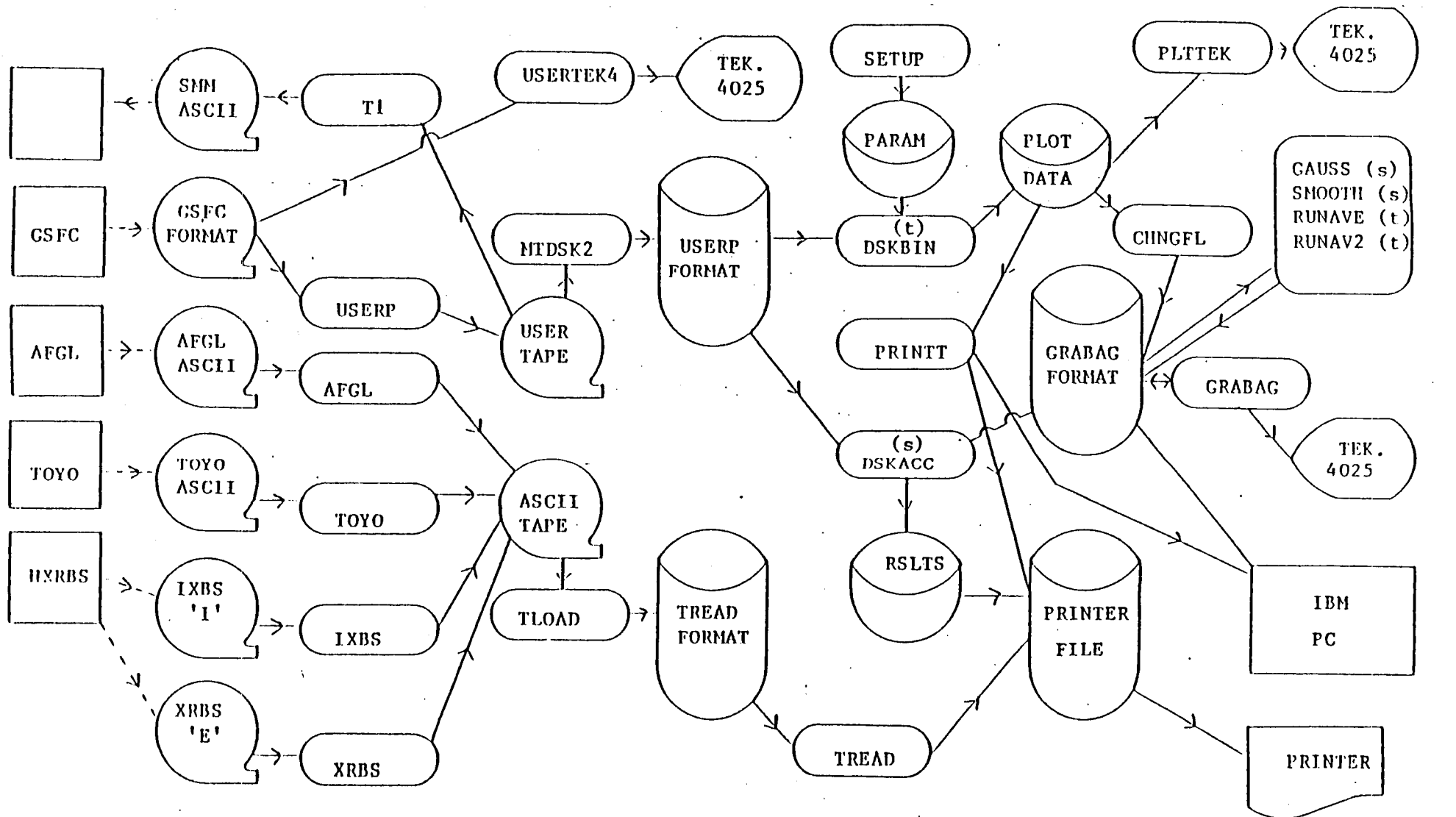
The SMM GRS data analysis software at UNH consists of a large number of independent programs. Each of these programs represent a step in the

process of transforming raw data (e.g. GSFC IPD tapes) into meaningful output. Figure 17 represents the data-flow process. This data analysis process was originally developed to be used in quick look fashion with both MPE and NRL designing more elaborate, user oriented analysis packages. Now that the Sun is in a period of minimal activity, we have begun to increase the longer range software usability by implementing a long term software analysis documentation and clean up project. This long term project consists of the following four steps:

1. Inventory all programs. Reduce their number by eliminating duplicates.
2. Increase integrity of analysis by having only one running source version of each program.
3. Fully document all running programs in a standardized fashion.
4. Begin to logically integrate programs to reduce the complexity of the analysis process.

A parallel task to this long term plan is the creation of two support documents which have been submitted to the Project office and NSDDC. The first document is user oriented. It will aid the prospective software applications user by outlining the function of each program, how it relates to the other programs, and how to go about using it. This document will outline the data analysis process in clear enough terms that it will facilitate, for any member of the scientific community, elementary data manipulation without rigorous training. The following is an outline of the major points covered within this document:

- present system configuration
- use of computing facility



(t) = TIME STUDIES

(s) = SPECTRAL STUDIES

GSFC = GODDARD SPACE FLIGHT CTR.
GREENBELT, MARYLAND

AFGL = AIR FORCE GEOPHYSICAL
LABORATORY, HANSCOM AIR FORCE
BASE, MASSACHUSETTS

HXRBS = GODDARD SPACE FLIGHT CTR.

Figure 17. SMM GRS Data Processing Flow Diagram

- purpose of analysis software
- use of each analysis program/package

The second document is concerned with the applications software from a software maintenance standpoint. This document will correspond directly, and be the result of, the documentation plans stated in step three above. This document will include documented versions of all running programs along with helpful flow diagrams and comments. In addition, this second document will also contain an indexed subroutine library with complete documentation on the use of each routine. The second document will contain the following main points:

- software design and documentation standards
- detailed description of Honeywell applications software
- detailed description of Honeywell utility software
- detailed description of IBM PC applications software
- indexed subroutine library

These documents are to be updated on a regular basis and will evolve along with the software. These two documents make up two out of three documents that make up the set of SMM GRS working documentation.

5. NATIONAL SPACE DATA AND DOCUMENTATION CENTER PLANS (NSDDC)

This contractual requirement is being satisfied in two steps.

1. Current SMM Data Center at Experimenters Operational Facility (EOF):
Archival microfilm data, prepared by NRL, has been sent to the GSFC

Experimenters Operation Facility (EOF) Data Center. This microfilm gives time history plots for all major data outputs of the SMM GRS and full gamma-ray spectra integrated in 5 minutes. Data was provided from turn-on, after launch, until August 1984. In addition, a listing of GRS events is being provided to the Data Center through Dave Speich, NOAA representative.

Any NSDDC user who needs information on a GRS event can obtain more information from the GRS Team at the University of New Hampshire, NRL or in Europe from the MPE.

The above procedure will be followed as long as the EOF and Data Center are operational or until space flight operations cease, whichever comes first.

2. Post EOF or Post Operations

The plan proposed to the SMM Project Scientist is briefly as follows:

- A. Supply microfilm with instructions for all data obtained from post-launch turn-on to the end of flight operations. (This item is currently being accomplished by NRL.)
- B. Provide copies of processed data tapes from IPD tapes obtained since post launch turn-on to end of flight operations. These tapes will be produced only for significant solar events and cosmic events.
- C. Provide an instrument manual and software manuals, sufficient for an independent user to develop analysis procedures for the SMM GRS. (The first versions of these three reports have been submitted to relevant NASA offices in March 1986.)
- D. Provide support to external users in interpreting SMM GRS data - funding permitting.

The above plan needs final approval by the SMM Project Scientist and SMM Project Manager, both for consent and additional funding where necessary.

6. GUEST INVESTIGATOR PROGRAM

In late 1985 NASA continued a Guest Investigator Program. We list briefly the Lead Scientist and his/her proposed program for the next year which bear directly on our experiment.

1. Principal Guest Investigator: Carol Jo Crannell
Goddard Space Flight Center

Program Title: A Proposal to Test Models of the Role of Energetic Particles with Radio, X-Ray, and Gamma-Ray Observations
2. Principal Guest Investigator: Robert B. Decker
Johns Hopkins University

Program Title: Numerical Studies of Particle Acceleration at Oblique, Turbulent, Coronal Shocks.
3. Principal Guest Investigator: Barry J. Geldzahler
Applied Research Corporation

Program Title: Search for Gamma-Ray Lines from SS433 Under the SMM GI Program.
4. Principal Guest Investigator: Barry J. Geldzahler
Applied Research Corporation

Program Title: Observations of 0.511 MeV Line Emission from the Direction of the Galactic Center.
5. Principal Guest Investigator: Mukul R. Kundu
University of Maryland

Program Title: Clark Lake Radioheliograph Observations in Support of SMM Experiments.

6. Principal Guest Investigator: Mukul R. Kundu
University of Maryland

Program Title: VLA and Westerbork Observations in Support of SMM Experiments.
7. Principal Guest Investigator: Kenneth R. Lang
Tufts University

Program Title: Simultaneous SMM and VLA Observations of the Sun.
8. Principal Guest Investigator: Mark E. Pesses
Applied Research Corporation

Program Title: The Rapid Acceleration of Ions in SMM Observed Solar Flares: Is it Shock Acceleration?
9. Principal Guest Investigator: Dean F. Smith
Berkeley Research Corporation

Program Title: Constraints on High Energy Flare Models Imposed by Radio, X-Ray, Gamma-Ray, and Interplanetary Observations.

7. AIR FORCE TASKS

The broad objectives of the Air Force task are basically the same as our primary NASA contract, that is to understand solar flare phenomena. However, it emphasizes correlation studies between ground-based flares and gamma-ray flares. The goal is to increase our ability to predict terrestrial effects from flares.

Our first efforts in this area showed a surprising lack of correlation between these ground-based measures of flare size with the flares' ability to produce gamma-ray emission. Thus, each of the correlations also

extended to gamma-ray production as observed by the SMM GRS and the solar energetic particles (SEPs) intensity measured in space near the Earth. This study is continuing on a more sophisticated basis with the hope of unraveling the original surprising result. In addition, a search for historical ground level monitor neutron events is in progress. The following collaborative papers describe work on this task.

1. Cliver, E.W., Forrest, D.J., McGuire, R.E., Von Rosenvinge, T.T. 1984, Proc. 18th Int. Cosmic Ray Conf. (Bangalore), 10, 334.
2. Cliver, E.W., Share, G.H., Chupp, E.L., Matz, S., Howard R. 1983, Bull 161st AAS Meet. (Boston), 14, 874. (Abstract)

8. REFERENCES

- Chupp, E.L. 1982, in Gamma Ray Transients and Related Astrophysical Phenomena, eds. Lingenfelter, R.E., Hudson, H.S., Worrall, D.M. (New York: AIP) p. 363.
- Chupp, E.L. 1983, Sol. Phys. **86**, 383.
- Chupp, E.L., Forrest, D.J., Heslin, J., Kanbach, G., Pinkau, K., et al. 1982, Ap. J. (Letters), **263**, L95.
- Chupp, E.L., Forrest, D.J., Share, G.H., Kanbach, G., Debrunner, H., et al. 1984. Proc 18th Int. Cosmic Ray Conf. (Bangalore), **10**, 334.
- Chupp, E.L., Forrest, D.J., Vestrand, W.T., Debrunner, H., Fluckiger, E., Cooper, J.F., Kanbach, G., Reppin, C. Share, G.H. 1985, to be presented at the 19th Icre, La Jolla, CA August 1985.
- Clayton, D.D. and Hoyle, F. 1974, Ap. J. (Letters) **187**, L101.
- Cliver, E., Share, G.H., Chupp, E.L., Matz, S., Howard, R. 1983, 161st Bull. AAS Meet., (Boston), **14**, 874. (Abstract)
- Cliver, E.W., Forrest, D.J., McGuire, R.E., Von Rosenvinge, T.T. 1984, Proc. 18th Int. Cosmic Ray. Conf. (Bangalore), **10**, 342.
- De Jager, C., De Jonge, G. 1978, Sol. Phys., **58**, 127.
- Debrunner, H., Fluckiger, E., Chupp, E.L., Forrest, D.J. 1984, Proc. 18th Int. Cosmic Ray Conf. (Bangalore), **4**, 75.
- Evenson, P., Meyer, P., Yanagita, S., Forrest, D.J. 1984, Ap. J., **282**, In press.
- Evenson, P., Meyer, P., Pyle, K.R. 1983, Ap. J., **274**, 875.
- Forrest, D.J. 1983, in Positron-Electron Pairs in Astrophysics, eds. Burns, M.L., Harding, A.K., Ramaty R. (New York: AIP), **101**, p. 3.
- Forrest, D.J., Chupp, E.L. 1983, Nature, **305**, 291.
- Gardner, B.M., Forrest, D.J., Zolcinski, M.C., Chupp, E.L., et al. 1981, Bull. Am. Astron. Soc. **13**(4), 903. (Abstract)
- Geldzahler, B.J., Share, G.H., Kinser, R.L., Forrest, D.J., Chupp, E.L., Reiger, E. 1985. Submitted to Ap. J.

- Hurley, K., Niel, M., Talon, R. 1983, Sol. Phys. 86, 367.
- Jacobson, A.S., et al. 1978, in **Gamma-Ray Spectroscopy in Astrophysics**, NASA TM-79619, 228.
- Kane, S. R., et al. 1986, Ap. J. 300, L95-L98.
- Kiplinger, A.L., Dennis, B.R., Emslie, A.G., Frost, K.J., Orwig, L.E. 1983, Sol. Phys. 86, 239. (Abstract)
- Kocharov, G.E. 1983, Invited Talks 8th Eur. Cosmic Ray Symp. (Bologna), p. 51.
- Leventhal, M., et al. 1974, Ap. J. 216, 491.
- Lingenfelter, R.E., Ramaty, R. 1967, in High Energy Nuclear Reactions in Astrophysics, ed. B.S.P. Shen, (New York: Benjamin) p. 99.
- Matz, S.M., Forrest, D.J., Vestrand, W.T., Chupp, E.L., Share, G.H., Rieger, E. 1985, Ap. J., 288, L37-L40.
- McGuire, R.E. 1983, Rev. Geophys. Space Phys. 21(2), 305.
- Murphy, R.J., Ramaty, R. 1985, Advances in Space Research, 4, 127.
- Murphy, R.J., et al. 1985. Presented at 19th ICRC, paper SH 2.1-13.
- Nakajima, H., Kosugi, T., Kai, K., Enome, S. 1983, Nature, 305, 292.
- Norris, J.P., et al. To be submitted to Ap. J. 1986.
- Prince, T.A., Forrest, D.J., Chupp, E.L., Kanbach, G., Share, G.H. 1984, Proc. 18th Int. Cosmic Ray Conf., (Bangalore), 4, 79.
- Ramaty, R., et al. 1975, Space Sci. Rec. 18, 341.
- Ramaty, R., Crannell, C.J. 1976, Ap. J., 203, 766.
- Ramaty, R., Kozlovsky, B., Lingenfelter, R.E. 1979, Ap. J. Suppl., 40, 487.
- Rieger, E., Reppin, C., Kanbach, G., Forrest, D.J., Chupp, E.L., et al. 1984, Proc. 18th Int. Cosmic Ray Conf., (Bangalore), 10, 338.
- Rieger, E., Share, G.H., Forrest, D.J., Kanbach, G., Reppin, C., Chupp, E.L. 1985, Nature, 312, 623.
- Share, G.H., Forrest, D.J., Chupp, E.L., Rieger, E. 1983, Bull. APS Meet. (Baltimore), 28, 730. (Abstract)
- Share, G.H., Chupp, E.L., Forrest, D.J., Rieger, E., 1983, in Positron-

Electron Pairs in Astrophysics, eds. Burns, M.L., Harding, A.K., Ramaty, R.
(New York: AIP) 101, p. 15.

Share, G.H., et al. 1985a, Ap.J. (Letters) 292, L61

Share, G.H., et al. 1985b, in preparation.

Starrfield, S., et al. 1972, Ap.J. 176, 169.

Truran, J.W., 1975, see Leventhal et al, 1977.

Van Hollebeke, M.A.I. 1979, Rev. Geophys. Space Phys., 17, 545.

Van Hollebeke, M.A., Ma Sung, L.S., McDonald, F.B. 1975, Sol. Phys.,
41, 189.

Vestrand, W.T., Forrest, D.J., Chupp, E.L., Rieger, E., Share, G.H., 1986,
Submitted to Ap. J.

Wang, H.T., Ramaty R. 1974, Sol. Phys. 36, 129.

Yoshimori, M., Hirasima, Y., Okudaira, K. 1983, Sol. Phys., 86, 375.

Yoshimori, M., Odudaira, K., Hirasima, Y., Kondo, I. 1984, Proc. 18th Int.
Cosmic Ray Conf. (Bangalore), 4, 85.